Coordination of host and endosymbiont gene expression governs endosymbiont growth and elimination in the cereal weevil *Sitophilus* spp.

Authors: Mariana Galvão Ferrarini[1,2], Agnès Vallier[3], Carole Vincent-Monégat[1], Elisa Dell'Aglio[1], Benjamin Gillet[4], Sandrine Hughes[4], Ophélie Hurtado[1], Guy Condemine[5], Anna Zaidman-Rémy[1], Rita Rebollo[3], Nicolas Parisot[1,*], Abdelaziz Heddi[1,*]

Affiliations
[1] Univ Lyon, INSA Lyon, INRAE, BF2I, UMR 203, 69621 Villeurbanne, France.
[2] Université de Lyon, Université Lyon 1, CNRS, Laboratoire de Biométrie et Biologie Evolutive UMR 5558, F-69622 Villeurbanne, France.
[3] Univ Lyon, INRAE, INSA Lyon, BF2I, UMR 203, 69621 Villeurbanne, France.
[4] Institut de Génomique Fonctionnelle de Lyon (IGFL), CNRS UMR 5242, Ecole Normale Supérieure de Lyon, Université de Lyon, Lyon, France.
[5] Univ Lyon, Université Lyon 1, INSA de Lyon, CNRS UMR 5240 Microbiologie Adaptation et Pathogénie, Villeurbanne, France.
* Corresponding authors NP: nicolas.parisot@insa-lyon.fr; AH: abdelaziz.heddi@insa-lyon.fr
Lead author: AH: abdelaziz.heddi@insa-lyon.fr

Abstract

Insects living in nutritionally poor environments often establish long-term relationships with intracellular bacteria that supplement their diets and improve their adaptive and invasive powers. Even though these symbiotic associations have been extensively studied on physiological, ecological and evolutionary levels, few studies have focused on the molecular dialogue between host and endosymbionts to identify genes and pathways involved in endosymbiosis control and dynamics. We simultaneously analyzed host and endosymbiont gene expression during the life cycle of the cereal weevil *Sitophilus oryzae*, from larval stages to adults, with a particular emphasis on emerging adults where the endosymbiont *Sodalis pierantonius* experiences a contrasted growth-climax-elimination dynamics. We unraveled a constant arms race in which different biological functions are intertwined and coregulated across both partners. These include immunity, metabolism, metal control, apoptosis, and bacterial stress response. Particularly, genes from the Hippo regulatory pathway are specifically induced by endosymbiont growth, while the regulation of metal ions constitutes the basis of the arms race between the two partners at the onset of the bacterial load climax. The study of these tightly regulated functions, which are at the center of symbiotic regulations, provides evidence on how hosts and bacteria finely tune their gene expression and respond to different physiological challenges constrained by insect development in a nutritionally limited ecological niche.

Graphical Abstract

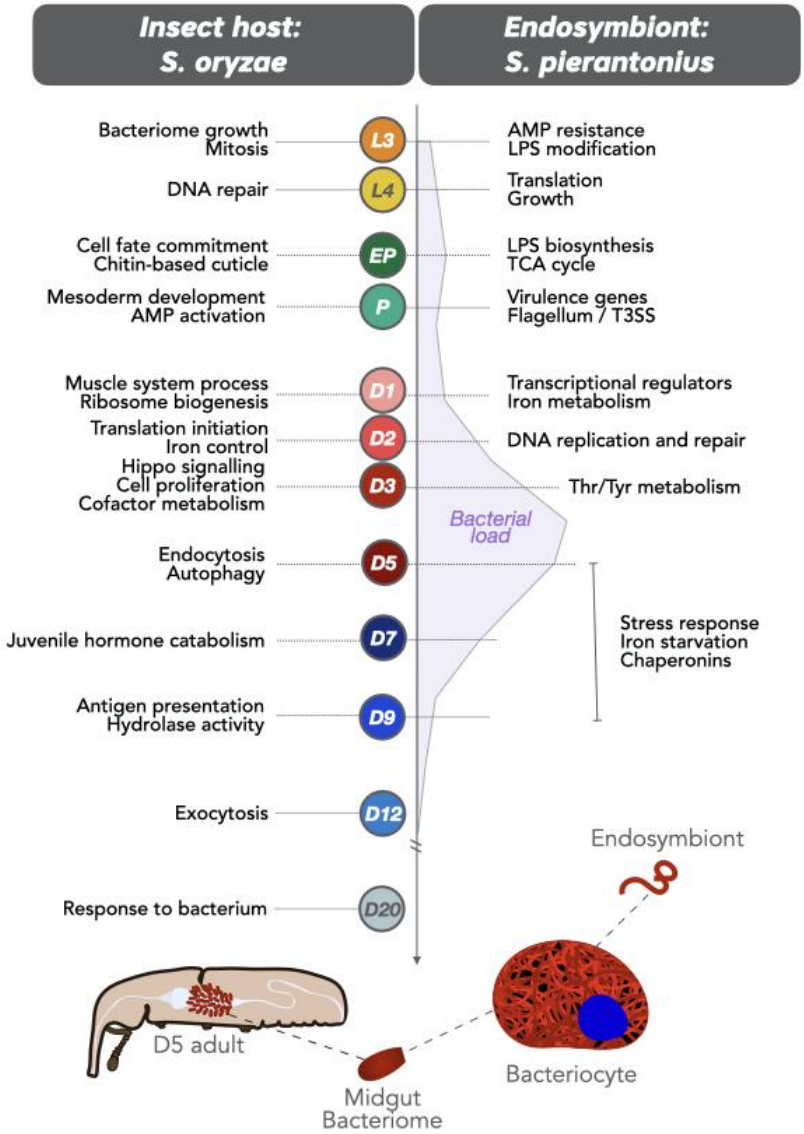

Introduction

One peculiar attribute of many insects thriving on nutritionally unbalanced niches, including insect pests and disease vectors, is their ability to establish long-term relationships with heritable intracellular bacteria.[1,2] These so-called endosymbionts supplement hosts with metabolic components lacking in their diets and are known to impact organisms in terms of genome evolution, reproduction, host ecology, metabolic exchanges, and immune functions.[3,4,5,6,7,8,9,10] In many species, endosymbiont distribution is restricted to female germ cells and bacteriocytes, which are specialized cells that can group into a bacteriome organ that secludes the bacteria and prevents their exposure to the host immune system.[11,12,13] These intimate relationships likely emerged from an ancestral infection of free-living bacteria, whose genomes experienced drastic size reduction, global enrichment in AT nucleic bases, and gene pseudogenization and deletion.[14,15,16,17,18,19,20] Moreover, vertically transmitted endosymbionts are under a relaxed evolutionary pressure due to a stable, nutritive and competition-free environment allowing for the accumulation of bacterial genome rearrangements and favoring host-symbiont co-evolution. This is highlighted by the loss of bacterial genes that become redundant or unnecessary in the new association, including virulence genes and genes encoding the bacterial cell wall elements,[21,22] by the loss or erosion of most transcriptional regulatory elements,[23,24] and by the increased metabolic interaction and complementation between the host and the endosymbiont.[1,21,25,26,27]

Even though the metabolic, ecological and evolutionary aspects of endosymbiosis have been well studied, the molecular mechanisms underlying the maintenance of endosymbionts and their regulation with respect to the host developmental needs, especially regarding the trade-off between bacterial burden and bacterial benefits, remain largely unexplored. This type of comprehensive study requires a one-to-one endosymbiont-host model system in which both the host and the bacteria are able to respond to different developmental constraints and biological stimuli with coordinated gene expression at critical stages of host development.

Endosymbiosis between the cereal weevil *Sitophilus oryzae* and the Gram-negative bacteria *Sodalis pierantonius* is most likely an exception among insects regarding several features. Contrary to their relatives, cereal weevils have established a symbiosis with *S. pierantonius* recently (<0.03 Myr).[28] Despite having lost many genes compared to free-living relatives, the genome of *S. pierantonius* has not undergone a massive erosion, as observed in old-lasting endosymbiotic bacteria, and encodes over 150 full-length regulatory proteins [19] as well as functional virulence factors.[29,30] In addition, the study of cereal weevils also have the advantage

of being associated solely with the *S. pierantonius* bacterium: most laboratory strains are free of Wolbachia, a common intracellular bacterium found in invertebrates,[31] and remarkably, no commensal bacteria have been identified within their guts so far. While *S. pierantonius* has never been cultivated successfully *in vitro*, weevils can be artificially depleted of the bacteria (aposymbiotic insects),[32] allowing for comparative studies between symbiotic and aposymbiotic insects with the same genetic background. Finally, the cell dynamics of *S. pierantonius* undergo a remarkably contrasted change during host development. Larval stages are considered homeostatic in relation to symbiotic load as the endosymbiont population grows slightly within a unique bacteriome, and bacteriocytes do not undergo any cellular or morphological changes. During metamorphosis, while bacteriocytes move along the midgut, endosymbionts infect stem cells that differentiate into new bacteriocytes forming numerous new bacteriomes at the apex of gut caeca.[29] In emerging adults, the endosymbiont population drastically increases (~5 fold in five days),[33,34] which was shown to be associated with metabolic requirements of the host while building its cuticle. Once the cuticle is achieved, the endosymbionts are eliminated and completely recycled in the course of 5 to 7 days. The midguts of young adults will remain devoid of bacteria throughout the rest of their lives. We have recently demonstrated the cost associated with such a drastic increase in bacteria load,[34] suggesting a balance between the metabolic requirements associated with cuticle synthesis, and the cost of harboring a large bacteria population. Here, we focus on understanding the shift in endosymbiont control associated with the increase in bacteria load along with the molecular signals directing endosymbiont elimination.

To identify host and bacterial coordinately expressed genes at different developmental conditions and constraints (i.e. larval-homeostasis, pupal endosymbiont-reinfection, adult-contrasted endosymbiont dynamics), we have conducted a host-symbiont metatranscriptomic approach (dual RNA-seq), and obtained high-throughput data simultaneously from both partners throughout 12 key stages of the weevil development. To pinpoint host genes whose expression is endosymbiont-dependent during young adult contrasted bacterial dynamics, we performed an additional comparative transcriptomic analysis between symbiotic and aposymbiotic insects. We show that larval stages are not transcriptionally stable as anticipated, marked by an enrichment in genes involved in cell growth from both host and bacteria. Following bacteriocyte migration, and while insects undergo metamorphosis, *S. pierantonius* activates secretion system and virulence genes, concomitantly with stem cell infection, bacteriocyte differentiation and antimicrobial peptide (AMP) encoding genes induction by the host. Metabolic and regulatory genes involved in this process are coordinated in both insect and bacteria. We identified several

signaling pathways and iron metabolism as symbiotic-specific features, and likely essential for bacterial growth. Once the bacterial benefit is over, insects activate recycling enzymes along with genes involved in apoptosis and autophagy. In response, bacteria activate stress-related-genes, including all cytoplasmic chaperones.

Overall, our findings show that interkingdom dialogue and coordinated regulation of gene expression play a pivotal role in the morphological reorganization of the bacteriome and the bacterial dynamics from larval stages to adulthood, highlighting adaptive features and sharply regulated biological functions to support both bacterial growth and recycling in emerging adults.

Material and methods

Animal rearing and sampling

In this study we used the *Sitophilus oryzae* strain Bouriz, which is Wolbachia-free and bears *Sodalis pierantonius* exclusively. Insects are reared on wheat grains at 27.5 °C and at 70 % relative humidity. Aposymbiotic animals were obtained by heat treatment and have been maintained in laboratory conditions similarly to the symbiotic line (Nardon et al., 1973). For the dual RNA-seq experiment, we sampled 12 time points for symbiotic insects during the insect development, namely: 3rd and 4th instar larvae (L3 and L4 respectively), early pupae (EP), pupae (P), along with eight time points into young adulthood starting from Day 1 to Day 20: D1, D2, D3, D5, D7, D9, D12, D20 (Figure 1B). Five time points were sampled for the regular RNA-seq in both symbiotic and aposymbiotic animals: D1, D3, D5, D7, and D9 (Figure 1C).

Bacteriomes were dissected in diethylpyrocarbonate-treated Buffer A (25 mM KCl, 10 mM $MgCl_2$, 250 mM sucrose, 35 mM Tris/HCl, pH = 7.5). For each replicate, bacteriomes (from 40 L3 and 30 L4) or midguts (from the remaining time points, ~15 insects for dual RNA-seq libraries, and 8-10 insects for each RNA-seq sample) were pooled, and stored at -80 °C before RNA extraction. Aposymbiotic sample replicates consisted of pools of 8-10 midguts from four time points: D1, D3, D7, D9.

RNA extraction, library preparation and sequencing for dual RNA-sequencing

Total RNA was extracted with TRIzol™ Reagent (Invitrogen ref.: 15596026) following the manufacturer's instructions. Nucleic acids were then purified using the NucleoSpin RNA Clean up kit (Macherey Nagel ref.: 740948). Genomic DNA was removed from the samples with the DNA-free DNAse kit (Ambion ref.: AM1906). Total RNA concentration and quality were checked using the Qubit Fluorometer (ThermoFisher Scientific) and Tapestation 2200 (Agilent Biotechnologies). Ribo-depletion and dual RNA-seq libraries were then performed with 100 ng of total RNA using the Ovation Universal RNA-seq System (NuGEN) following the manufacturer's instructions and sequenced on a NextSeq 500 instrument (Illumina) at the sequencing platform of the Institut de Génomique Fonctionnelle de Lyon, Ecole Normale Supérieure de Lyon, France. Supplementary Figure S1A explains the schematic pipeline for the dual RNA-seq.

RNA extraction for host RNA-sequencing

Total RNA was extracted using the Qiagen Allprep DNA/RNA micro kit (Qiagen ref.: 80284) following the manufacturer's protocol. RNA quality assessment and library preparation was performed at the GenomEast platform at the Institute of Genetics and Molecular and Cellular Biology using Illumina Stranded mRNA Prep Ligation (Reference Guide - PN 1000000124518). RNA-Seq libraries were generated according to manufacturer's instructions from 200 ng of total RNA using the Illumina Stranded mRNA Prep, Ligation kit and IDT for Illumina RNA UD Indexes Ligation. Libraries were sequenced on an Illumina HiSeq 4000 sequencer as paired-end 100 base reads.

Preprocessing, mapping of reads and differential expression analysis

Supplementary Figure S1B depicts the processing and bioinformatic analyses. The raw reads from both sequencing methods (dual RNA-seq and RNA-seq) were processed using CUTADAPT v1.18[35] to remove adapters, filter out reads shorter than 50 bp and reads that had mean quality of 30 or less. The clean reads were mapped against the *S. oryzae* genome (GCF_002938485.1) with STAR v2.7.3a[36] and S. *pierantonius* (CP006568.1) with BOWTIE v2.3.5[37] when suitable. Supplementary Table S1 presents all information regarding the number of raw reads, trimming and mapping to each of the genomes (when suitable) for both sequencing methods. Shared reads from dual RNA-seq between the two genomes were filtered out with the aid of SAMTOOLS[38] and PICARD (available from https://broadinstitute.github.io/picard/). The high proportion of multi-mapped reads from both genomes is explained by the high abundance of repeats in both *S. oryzae*[39] and *S. pierantonius*[19] (74% of repeats in *S. oryzae* and 19% of insertion sequences in *S. pierantonius*). Gene counts were obtained for uniquely mapped reads with FEATURECOUNTS v2.01 method from the SUBREAD package[40] (Supplementary Tables S2 and S3 for host and endosymbiont dual RNA-seq results respectively). The SARTOOLS package[41] was used for quality assessment of samples and pairwise differential expression analyses using the DESEQ2 v1.34.0.[42] After testing, the p-values were adjusted with the Benjamini-Hochberg[43] correction for multi-testing. Genes were considered differentially expressed when adjusted p-values < 0.05 (results for differential expression of the dual RNA-seq data are provided in Supplementary Tables S4 and S5). Each time point was tested against all time points to construct an overall gene expression graph, however, we looked closely at the results between two successive time points (t versus its previous time point $t - 1$). Since we had a high number of conditions and pairwise comparisons tested within the dual RNA-seq dataset, we also performed a likelihood ratio test (LRT) in order to create a reduced model and detect which genes were the most significantly

expressed throughout all time points (Supplementary Table S6 and S7). For the regular host RNA-seq, counts are provided in Supplementary Table S8. A comparison with the previous time point as well as a linear model were performed with DESEQ2 using the following design: ~time+symbiont+interaction (Supplementary Table S9). Inspection of all DEGs was performed to verify the variability between samples intra-condition. The clustering of samples and PCA analysis are provided in Supplementary Figure S2 and S3.

Clustering and profiling analyses

The standardized expression (normalized to mean zero and standard deviation one) of DEGs (adjusted p-value < 0.05) of both insect and bacteria were loaded into MATLAB v9.12.0 R2022a and separately clustered using a temporal clustering by affinity propagation with the method TCAP v.2.[44] The results were then loaded and analyzed in R v4.1.2[45] and clusters with at least 0.8 of mean similarity which presented similar profiles but differed mainly by the magnitudes of expression were merged into superclusters using Euclidean distance with the PHEATMAP package v.1.0.12.[46] Clusters with less than 10 genes were discarded and visualization of profiles was made with GGPLOT2 package v3.3.6.[47] Supplementary Tables S10 and S11 present the clustering results for the host and endosymbiont respectively from the dual transcriptomics dataset and Supplementary Table S12 presents the clustering results for the host RNA-seq data between symbiotic and aposymbiotic adults.

Functional enrichment analysis

Functional analysis took into account as input the lists of DEGs and superclusters. We performed a global functional enrichment analysis using Cluster Profiler[48] with multi-testing correction[43] in R to find out which functions were over-represented in each comparison. Gene Ontology[49] (GO) terms and KEGG[50] pathways with adjusted p-values < 0.05 were defined as significantly enriched. We also visualized biological pathways that were highly impacted in both insect and bacteria, by projecting the transcriptomic data onto the online platform Search and Color from KEGG. When needed, GO terms were reduced to representative non-redundant terms with the use of the REVIGO tool.[51] Results for the dual RNA-seq dataset are provided in Supplementary Tables S13 and S14 for both host and endosymbiont. Results for the RNA-seq dataset are provided in Supplementary Table S15.

Results and Discussion

One of the typical features of weevil endosymbiosis (Figure 1A), with regards to other insect relatives, is the contrasted endosymbiont dynamics in young adults. Following adult metamorphosis and gut stem cell infection, the bacterial population grows exponentially for a few days, concomitantly with the biosynthesis of the insect's cuticle, and soon after the bacteria are actively recycled by the host. At 10-12 days of adulthood, laboratory-reared insects are almost entirely devoid of midgut bacteria.[33] Thus, at least three distinct developmental constraints can be distinguished after metamorphosis: initial bacterial growth concomitant to bacterial benefit, climax of bacterial load, and subsequent symbiont elimination once bacterial burden overcomes the benefits.

To identify host and bacterial genes and pathways involved in bacterial growth regulation, we have established a host-symbiont transcriptomic approach (dual RNA-seq), resulting in high-throughput data simultaneously on both partners. We have analyzed insect and bacterial gene expression at 12 key stages of the weevil development, from 3rd instar larvae to 20-day-old adults (Figure 1B). To pinpoint endosymbiont-dependent gene expression, we performed an additional transcriptomic comparison between symbiotic and artificially obtained aposymbiotic insects (Figure 1C).

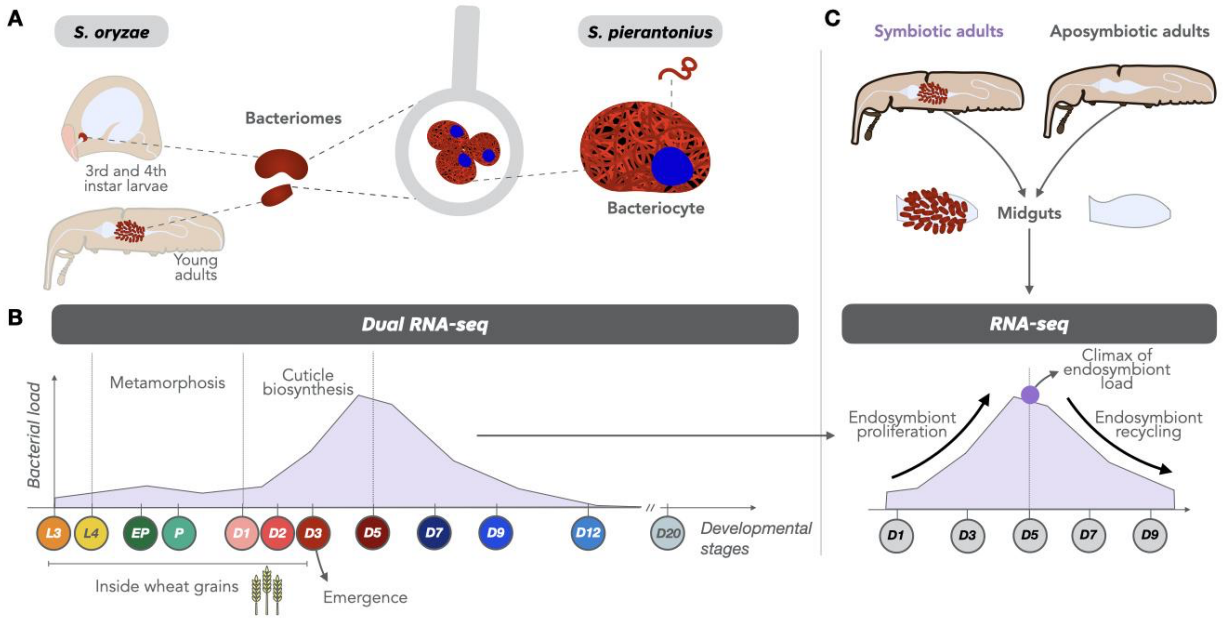

Figure 1. Experimental design for deciphering the molecular dialogue between *Sitophilus oryzae* and its endosymbiont *Sodalis pierantonius*. (A) Schematic illustration of the bacteriome location in larvae and adult weevils. (B) Key developmental life stages sampled in this study for the dual RNA-seq and schematic of gut bacterial load from previous studies.[33,34] (C) Time points sampled for the RNA-seq comparison of symbiotic and aposymbiotic weevils. Arrows depict the increase in bacterial load during the first days of adulthood, followed by the drastic recycling of endosymbionts. L : larvae, EP : early pupae, P: pupae, DX, estimation of the adult age in days.

The dual RNA-seq recovered reads successfully from both insect and bacteria, ranging from 120 M to 200 M reads per sample (Supplementary Table S1). Depending on the tissue and time point, and in accordance with the bacterial load dynamics, the percentage of reads mapping to the bacteria varied from 8% of total trimmed reads (for L3 and L4) to less than 0.5% (~0.39% in D12 and ~0.07% in D20). The higher mapping of reads in L3 and L4 compared to later stages, is explained mainly by the difference in tissue composition. While larval bacteriomes can be easily dissected from the fore-midgut junction, pupal and adult bacteriomes are tightly associated with the midgut and hence dual RNA-seq was conducted on dissected guts containing bacteriomes (Figure 1A). Focusing only on young adult bacterial reads, their proportion varies in accordance to the previously described bacterial load (Figure 1B and Supplementary Figure S4), denoting an overall correlation between bacterial load and bacterial gene expression. Due to the extremely low bacterial load at D12 and D20, we were not able to perform differential expression analysis at these time points for *S. pierantonius*.

The number of differentially expressed genes (DEGs) varied drastically in both weevils and endosymbionts (Supplementary Tables S4 and S5). For insect genes, DEGs ranged from 38 (between D12 and D9) to 6229 (between D1 and P), as presented in Table 1. The major shift in

expression observed during metamorphosis had been previously reported between L4 vs early pupae developmental stages,[29] due to the extreme tissue rearrangements. Here, we monitored an even higher number of DEGs than previously, especially regarding the endosymbiont, thanks to the deeper sequencing obtained for this study. After the bacterial elimination period (D12 and D20), the expression of insect genes is stable, with nearly no DEGs between D12 vs D9, nor D20 vs D12. As for the endosymbiont, up to 468 genes were differentially expressed between D1 and P. Even between L3 and L4 larval stages, which were considered as homeostatic with regard to symbiosis due to the coordinated growth of the bacterial population and the bacteriome tissue, a significant number of DE genes from both partners were observed, attesting that *S. pierantonius* gene expression is regulated and responds to different developmental conditions.

Table 1. Number of DEGs detected for *S. oryzae* and *S. pierantonius* throughout 12 time points during the insect's life cycle. Genes were considered as differentially expressed when the adjusted P-value was lower than 0.05 and the absolute Log2 of fold change was greater than 0.5.

Comparison	***Host Up-regulated***	***Host Down-regulated***	***Endosymbiont Up-regulated***	***Endosymbiont Down-regulated***
L4 vs L3	915	1568	98	64
EP vs L4	3462	2301	115	97
P vs EP	1948	1016	162	196
D1 vs P	3032	3197	177	291
D2 vs D1	491	261	13	8
D3 vs D2	1002	989	82	134
D5 vs D3	81	265	114	142
D7 vs D5	71	276	10	8
D9 vs D7	36	114	3	0
D12 vs D9	2	36		
D20 vs D12	29	65		

Based on the centered normalized expression of DEGs, we conducted a clustering analysis of genes presenting similar profiles with TCAP2.[44] Finally, clusters of genes having similar expression but different magnitudes were further merged into superclusters (Supplementary

Tables S10 and S11). The overall results of selected superclusters throughout the developmental stages from both host and endosymbiont are depicted in Figure 2 (Supplementary Figures S5 and S6 provide complete profiles of all superclusters). Superclusters composed by genes from the insect will be denoted as **SO** followed by the supercluster number; whereas superclusters composed by genes from the endosymbiont will be denoted with an **SP** followed by the number of the supercluster. Functional enrichment of the final superclusters (Supplementary Tables S13 and S14) unraveled several biological functions during most of the stages of the developmental process and will be discussed in the following subsections. The main enriched functions, along with the expression of an insect gene (or in the bacterial side, gene and/or operons) related to such functions are depicted in Figure 2. Gene names or abbreviations mentioned throughout the next sections in the main text or within figures are provided with the respective IDs in Supplementary Table S16.

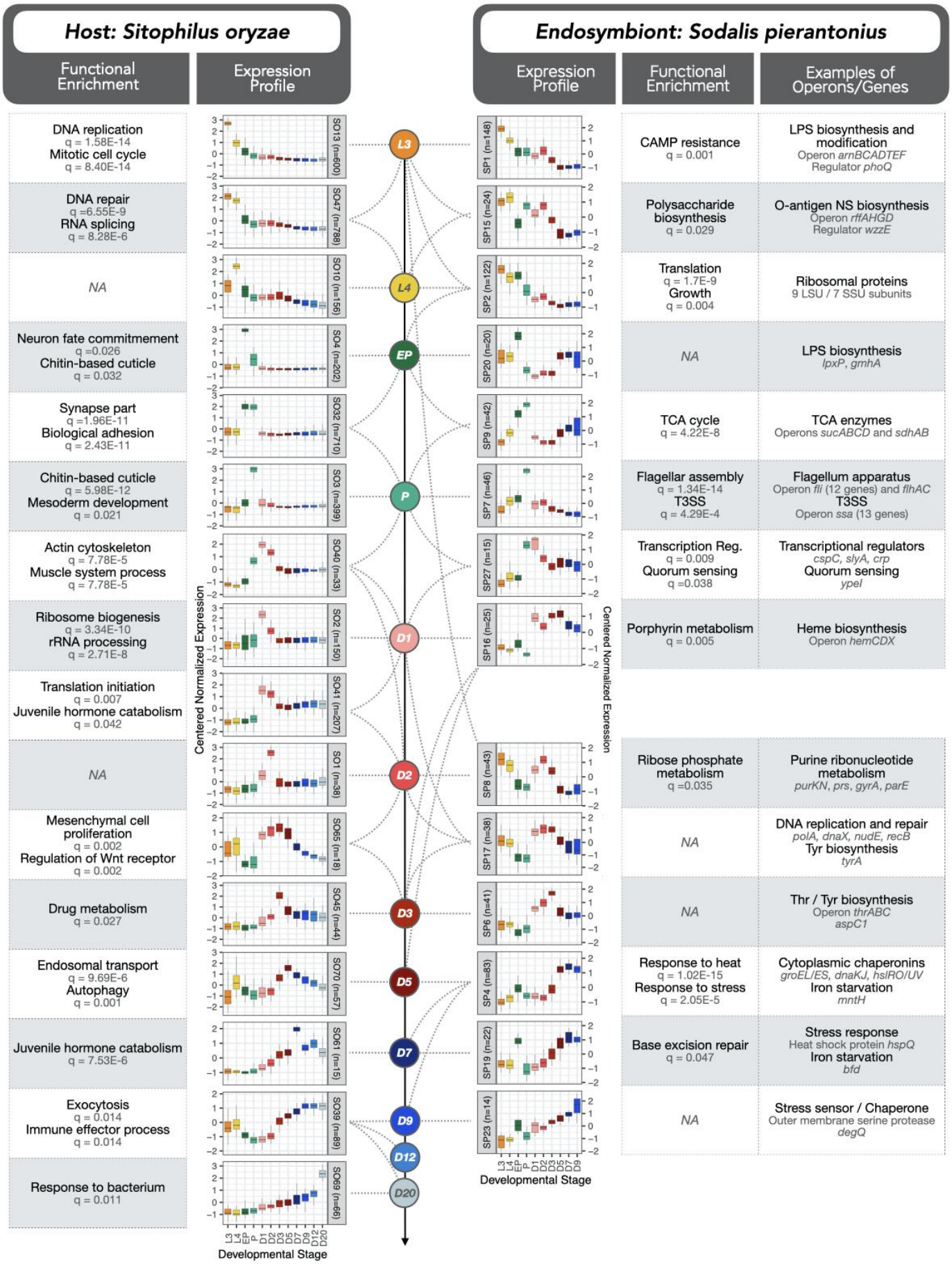
Host: Sitophilus oryzae
Functional Enrichment
Expression Profile
DNA replication
q = 1.58E-14
Mitotic cell cycle
q = 8.40E-14
DNA repair
q =6.55E-9
RNA splicing
q = 8.28E-6
NA
Neuron fate commitmement
q =0.026
Chitin-based cuticle
q = 0.032
Synapse part
q =1.96E-11
Biological adhesion
q = 2.43E-11
Chitin-based cuticle
q = 5.98E-12
Mesoderm development
q = 0.021
Actin cytoskeleton
q = 7.78E-5
Muscle system process
q = 7.78E-5
Ribosome biogenesis
q = 3.34E-10
rRNA processing
q = 2.71E-8
Translation initiation
q = 0.007
Juvenile hormone catabolism
q = 0.042
NA
Mesenchymal cell proliferation
q = 0.002
Regulation of Wnt receptor
q = 0.002
Drug metabolism
q = 0.027
Endosomal transport
q = 9.69E-6
Autophagy
q = 0.001
Juvenile hormone catabolism
q = 7.53E-6
Exocytosis
q = 0.014
Immune effector process
q = 0.014
Response to bacterium
q = 0.011
SO13 (n=600)
SO47 (n=788)
SO10 (n=156)
SO4 (n=202)
SO32 (n=710)
SO3 (n=399)
SO40 (n=33)
SO2 (n=150)
SO41 (n=207)
SO1 (n=38)
SO65 (n=18)
SO45 (n=44)
SO70 (n=57)
SO61 (n=15)
SO39 (n=89)
SO69 (n=66)
Centered Normalized Expression
L3 L4 EP P D1 D2 D3 D5 D7 D9 D12 D20
Developmental Stage
L3
L4
EP
P
D1
D2
D3
D5
D7
D9
D12
D20
Endosymbiont: Sodalis pierantonius
Expression Profile
Functional Enrichment
Examples of Operons/Genes
SP1 (n=148)
SP15 (n=24)
SP2 (n=122)
SP20 (n=20)
SP9 (n=42)
SP7 (n=46)
SP27 (n=15)
SP16 (n=25)
SP8 (n=43)
SP17 (n=38)
SP6 (n=41)
SP4 (n=83)
SP19 (n=22)
SP23 (n=14)
Centered Normalized Expression
L3 L4 EP P D1 D2 D3 D5 D7 D9
Developmental Stage
CAMP resistance
q = 0.001
LPS biosynthesis and modification
Operon arnBCADTEF
Regulator phoQ
Polysaccharide biosynthesis
q = 0.029
O-antigen NS biosynthesis
Operon rffAHGD
Regulator wzzE
Translation
q = 1.7E-9
Growth
q = 0.004
Ribosomal proteins
9 LSU / 7 SSU subunits
NA
LPS biosynthesis
lpxP, gmhA
TCA cycle
q = 4.22E-8
TCA enzymes
Operons sucABCD and sdhAB
Flagellar assembly
q = 1.34E-14
T3SS
q = 4.29E-4
Flagellum apparatus
Operon fli (12 genes) and flhAC
T3SS
Operon ssa (13 genes)
Transcription Reg.
q = 0.009
Quorum sensing
q =0.038
Transcriptional regulators
cspC, slyA, crp
Quorum sensing
ypeI
Porphyrin metabolism
q = 0.005
Heme biosynthesis
Operon hemCDX
Ribose phosphate metabolism
q =0.035
Purine ribonucleotide metabolism
purKN, prs, gyrA, parE
NA
DNA replication and repair
polA, dnaX, nudE, recB
Tyr biosynthesis
tyrA
NA
Thr / Tyr biosynthesis
Operon thrABC
aspC1
Response to heat
q = 1.02E-15
Response to stress
q = 2.05E-5
Cytoplasmic chaperonins
groEL/ES, dnaKJ, hslRO/UV
Iron starvation
mntH
Base excision repair
q = 0.047
Stress response
Heat shock protein hspQ
Iron starvation
bfd
NA
Stress sensor / Chaperone
Outer membrane serine protease
degQ

Figure 2. Dual RNA-seq expression profiles of both host and endosymbiont during the 12 stages of development studied. Profiles highly induced in each of the stages (or in more than one stage at times) are indicated with dashed lines. Host profiles are indicated with SO (for *Sitophilus oryzae*) followed by the profile number whereas endosymbiont profiles are indicated with SP (for *Sodalis pierantonius*) followed by the profile number. Each profile was built based on the expression of different numbers of genes (indicated by *n*). Functional enrichment of each profile based on GO and KEGG is indicated on the left side for host genes and on the right for endosymbiont genes. We also provide, on the far right, examples of endosymbiont genes belonging to each profile. The complete set of profiles built is provided in Supplementary Figures S5 and S6.

Larval stages show active cell growth in both host and endosymbiont

When compared to pupal and adult stages, genes highly expressed in larval bacteriomes show a significant functional enrichment related to mitosis, nuclear division, mitochondrion, ribosome, RNA splicing, nucleolus, DNA repair, and protein refolding, suggesting a high proliferation of cells, especially at the L3 stage (superclusters SO13, SO47 and SO10 from Figure 2; SO28 from Supplementary Figure S5). These results support the idea that the larval bacteriome is in a growing phase, presumably storing up energy and metabolites before insects stop feeding and start metamorphosis. The gene *tor,* a serine/threonine protein kinase that regulates and promotes cell and tissue growth in *Drosophila*,[52] is highly induced at L4 stage (supercluster SO10), along with bacterial genes involved in ribosome synthesis and translation, gene expression, growth, cell wall, and lipopolysaccharide (LPS) biosynthesis (superclusters SP1, SP2 and SP15), concomitantly with a slight increase in bacterial load from L3 to L4. The most significant gene from the whole bacterial dataset is an LPS biosynthesis gene, namely *murB* (p-adj = 1.09E-277, Supplementary Table S7), whose expression is very high at L3, and drops more than 40 folds by D9.

A complete bacterial operon (*arn*) acting on LPS modification through the addition of 4-amino-4-deoxy-l-arabinose to the outer membrane lipid A moiety and cationic antimicrobial peptide (CAMP) resistance was also induced at larval stages (supercluster SP1). This operon has previously been shown to be involved in increased antimicrobial peptide (AMP) resistance of the pathogenic free-living bacteria *Dickeya dadantii*,[53] when infecting the pea aphid *Acyrthosiphon pisum*. The *arn* operon, along with several other virulence response mechanisms, was described to be regulated by the PhoP/PhoQ proteins.[54] Here, genes encoding the PhoP/PhoQ system show higher expression at larval stages (*phoQ*, supercluster SP1, Figure 2 and *phoP*, supercluster SP2, Supplementary Figure S6), with the *phoQ* gene expression being the second most significant within the entire bacterial dataset (p-adj = 3.04E-266, Supplementary Table S7). At first sight, these results look intriguing when considering that endosymbionts are generally isolated from the

host immune system and inhabit a stable environment where the requirement for sensory functions is expected to be relaxed or absent. Nevertheless, previous work on *Sodalis glossinidius*, the secondary endosymbiont of the tsetse fly which experiences both extra- and intracellular life-styles, showed that the PhoP/PhoQ system is required for the bacterial survival within the insect host by mediating the expression of genes involved in resistance to host AMPs.[55] This system was shown to be necessary for the transition from free-living to obligate endosymbiosis status in the tsetse fly .[54] It is important to notice that while the PhoP/PhoQ system could be essential in extracellular conditions in *S. glossinidius*, *S. pierantonius* is strictly intracellular during all weevil larval stages. Remarkably, all AMP encoding genes are downregulated within the weevil's bacteriocytes, with the notable exception of the coleoptericin A (ColA), which continuously targets endosymbionts and inhibits their cell division.[56,11] The PhoP/PhoQ system activation in L3 and L4 may be connected to *colA* specific expression in bacteriomes.

Six bacterial genes from the ATP synthase operon (*atpEAGDBH*) also belong to the superclusters SP1, SP2, SP8, and SP15, showing high expression in larval stages. Previous biochemical studies have reported that weevil mitochondrial specific enzymatic activities are higher in symbiotic than in aposymbiotic larvae.[57,58] Here, we provide further evidence that the increase in host mitochondrial activity is part of a coordinated regulation from bacteria and host to generate energy necessary for an active metabolism within the bacteriocytes and endosymbiont cells.

Finally, it has been recurrently suggested that the larval bacteriome is at a homeostatic state between the host and endosymbiont, since bacterial growth is not significantly important, bacteriocytes do not undergo cellular rearrangements, and the host immune response is downregulated, with the notable exception of ColA.[13,29] Here, we show that such an equilibrium involves both the host and the endosymbiont by setting in motion the physiological and energetic needs necessary for insect metamorphosis, along with bacteriocyte migration and differentiation of new bacteriomes during the pupal stages. In sum, while the larval bacteriome exhibits a homeostatic status with regard to bacterial dynamics and bacteriocyte cellular processes, this work reveals that host and bacterial coordinated gene expression precedes energy production and components synthesis, necessary for host metamorphosis execution and completion.

Metamorphosis and AMP expression depict an arms race between symbiotic partners

During metamorphosis, the single larval bacteriome disassembles, bacteriocytes migrate along the midgut, and bacteria infect new stem cells at the apexes of midgut caeca, which differentiate further into novel bacteriocytes that group into several bacteriomes around the midgut of the young adult.[29] As expected, and in accordance with our previous observations, insect genes highly expressed in pupal stages were overall enriched in cell adhesion, mesodermal cell commitment, chitin based-cuticle (gene *cp-67*, coding for the cuticle protein 67) and synapse (gene *syp-1*, coding for synaptotagmin 1) (superclusters SO3, SO4, and SO32 in Figure 2; SO9 and SO11 from Supplementary Figure S5). Concomitant to the insect's metamorphosis, the bacteria showed an increased expression in TCA cycle, and several virulence-related genes (superclusters SP7 from Figure 2, SP10 from Supplementary Figure S6), in agreement with our previous work.[29] Virulence genes included the partially degraded operons of the flagellum apparatus (operons *fli* and *flh*), and type III secretion system (T3SS, operon *ssa* and *sseE*). No apparent effector for the T3SS was ever reported in *S. pierantonius*. Here, we have detected a pseudogene highly expressed in pupal stage exclusively, homolog to the *Salmonella typhimurium* deubiquitinase SseL, a T3SS known effector[59] (Supplementary Figure S7). Despite a premature stop codon, the *S. pierantonius sseL* gene presents an intact peptidase domain. SseL inhibits autophagic clearance of cytoplasmic aggregates that form during *Salmonella* infection in epithelial cells, favoring intracellular bacterial replication.[60] The upregulation of *sseL* during the weevil's metamorphosis suggests an essential role for the infective behavior of *S. pierantonius*.

We have also detected a spike in 10 insect AMP genes during metamorphosis, namely *coleoptericin-A*, *coleoptericin-B*, *acanthoscurrin-1-like*, *cathelicidin-like antimicrobial protein*, *cecropin*, *diptericin-2*, *diptericin-3*, *diptericin-4*, *gly-rich AMP-like*, and *holotricin-3-like*, (Supplementary Figure S8). It is appealing to hypothesize that this increase in AMP expression concomitant to the process of bacterial infection of stem cells is either (i) a response of the host to the virulent bacteria exiting the bacteriocytes or ii) it might be part of a developmental program and independent of the bacterial interaction. Even though AMP genes are usually induced upon infection, there is growing evidence suggesting they are activated at specific developmental stages regardless of the presence of a bacterium.[61,62] Moreover, AMPs in sub-lethal concentrations were also shown to trigger a strong restructuring effect on gene expression in other bacteria.[63,64]

This peak of AMP expression during metamorphosis denotes a different profile of expression than the one of the cationic antimicrobial peptides (CAMP) resistance reported in the previous section within the bacteria. The only AMP known to be chronically expressed within bacteriocytes and guarantee tissue homeostasis is the Coleoptericin A (ColA), while other AMPs are thought to be secreted outside the bacteriome tissue.[13] In this work, the only AMP highly expressed in larval bacteriomes, and whose expression parallels the profile of bacterial load in adult stages, is a partial Diptericin-like (gene *dpt-like partial*, belonging to cluster SO47). This gene, unlike the other *diptericin* genes, lacks the 5' end that encodes for a signal peptide for export[39] and is therefore predicted to be intracellular and likely resides within bacteriocytes, similarly to ColA.

In conclusion, in addition to *colA*, nine AMPs were shown to be upregulated precisely during metamorphosis, suggesting that novel immune regulators might be involved in a developmental-specific manner. We also pinpointed a novel *diptericin-like* whose expression parallels bacterial load, and, contrary to most AMPs, is predicted to reside within bacteriocytes, and is likely involved in endosymbiont regulation.

Early stages of adulthood depict active tissue and bacterial growth and coordinated metabolism

As we previously mentioned, there are three important features of bacterial dynamics tightly regulated during the young adult developmental stages: endosymbiont proliferation, climax in bacterial load and subsequent bacterial recycling. We recently showed that endosymbiont proliferation relies on metabolic regulation and the availability of carbohydrates from diet intake, and this proliferation seems to escape host control.[34] In contrast, both the bacterial load climax and subsequent recycling were described to be genetically controlled by the host,[65,33] even though the specific genes orchestrating these features remain unknown. Thus, our main focus in the following sections was to identify genes and pathways involved in bacterial dynamics, along with the coordinated bacterial responses to host changes.

While weevils mainly feed on complex polysaccharides from cereal grains, such as starch and cellulose, symbiotic bacteria generally uptake derived carbohydrates, mostly converted to monosaccharides. We previously predicted which metabolites were exchanged during the initial stages of adulthood based on the complete genomes of both partners,[19,39] and pinpointed, in addition to monosaccharides, essential amino acids, cofactors and nucleotide precursors.[39] Host genes enriched at the initial stages of adulthood (D1 and D2), prior to insect emergence from the

grain (superclusters SO1, SO2, SO40, SO41, from Figure 2; SO16, SO54, and SO55 from Supplementary Figure S5), had a significant functional enrichment related to ribosome biogenesis, rRNA processing, actin cytoskeleton, muscle system process, suggesting tissue development (especially at D1) before imminent feeding and emergence from the grain. We recently showed that at D1, insects are motionless and unable to feed,[34] a process that takes place at D2. Our data point to the synthesis of novel proteins necessary for midgut food uptake and muscle peristaltic contraction. Other functions activated at these initial stages of adulthood are juvenile hormone catabolism, indicating the end of metamorphosis, and hydrolase activity, including glycosidases, a pectinesterase, endoglucanases and an exoglucanase B - *exgB*, showing that the degradation of cellulose and other insoluble plant cell wall sugars might be essential, in addition to starch inside the grains. Concomitantly and before emergence, a pectin degradation protein encoding gene is induced in bacteria at D1. Moreover, at the N stage, a complete pathway for the degradation of galacturonate - the pectin monomeric unit (*uxaABC*), along with two known regulators of these functions (*uxuR* and *kdgR*) in other bacteria[66,67,68] also present an increased expression.

Remarkably, bacterial gene enrichment analysis (superclusters SP8, SP16, SP17) showed a host-endosymbiont coordination in the biosynthesis and metabolism of other precursors necessary for growth. This includes the activation of DNA replication and repair along with the biosynthesis of heme and metabolism of ribonucleotides from D1 to D3. Particularly at D1, we noticed an increased expression of bacterial transcription factors (supercluster SP27), and therefore a general transcriptional activation, suggesting that even though the insect is not feeding until shortly before emergence from the grain, the bacteria seem to be not directly affected by this lack of resources, probably relying on stored metabolic components during the last larval stages. From D3 onwards, the bacteria proliferate inside the growing bacteriocytes and actively produce essential metabolites necessary for the host.[39] Metabolism is usually regulated in a straightforward manner, in which the availability of a substrate or the lack of a product in a certain pathway induces the expression of key genes in such a pathway. This equilibrium becomes more complex when dealing with two distinct organisms, coming from different kingdoms of life, but a great example of this regulation are the essential amino acids threonine and tyrosine, provided to the host by the endosymbiont.[39] We show that the operon *thrABC* (threonine synthase) and the genes *aspC1* and *tyrA* (tyrosine biosynthesis) are induced after metamorphosis with a peak at D2/D3 (superclusters SP6 and SP17). This suggests that the provision of such essential amino acids, along with other cofactors, from the endosymbiont to the host, initiates before the insect

leaves the grain and likely helps the insect to anticipate the cuticle synthesis and mouthparts acquisition during the fasting period. The tyrosine amino acid is particularly critical since it is one of the main precursors of the dihydroxyphenylalanine (DOPA), an essential component of the insect's cuticle synthesis,[33] which is fully completed around D5 in weevils. A supercluster from the host with a higher expression from D1 to D5 (SO65), had enriched terms related to mesenchymal cell proliferation and stem cell maintenance, suggesting gut and bacteriome tissue growth until the cuticle is completed. The two copies of the division abnormally delayed-like genes (*dally*) belong to this supercluster. Dally and Dally-like proteins are two major heparan sulfate proteoglycans from *Drosophila*, and heparan sulfate itself is known to negatively regulate intestinal stem cell proliferation.[69] Interestingly, a final up-regulation of genes belonging to the juvenile hormone catabolism was detected around D7 (an example is the carboxylesterase *vest-6*, supercluster SO61), likely depicting the insect's maturation after the completion of the cuticle.

To uncover host genes that are modulated by the endosymbiont, we performed a regular eukaryotic RNA-seq between gut tissues dissected from symbiotic and aposymbiotic insects at five key stages of the young adulthood (D1, D3, D5, D7, and D9, as presented in Figure 1B). We performed a DEG analysis and detected that the presence of the endosymbiont was the major effect controlling either the induction or the depletion of gene expression throughout the dataset (Supplementary Figure S9). Similarly to the dual RNA-seq analysis, we combined clusters from symbiotic and aposymbiotic insects into Superclusters (Figure 3, and Supplementary Figures S10 and S11), by taking into account their expression profiles and the stages in which we detected a differential expression between symbiotic and aposymbiotic weevils (Supplementary Table S10). Functional enrichment was performed (Supplementary Table S15) and superclusters induced in symbiotic adults will be denoted with an S, whereas superclusters induced in aposymbiotic insects with an A.

In agreement with the findings that endosymbiont proliferation relies on the availability of carbohydrates from food intake,[34] genes upregulated in all symbiotic stages were enriched in transport of carbohydrate functions (Supercluster S1; Figure 3). Interestingly, pentose interconversion and cofactor metabolism genes were induced specifically in symbiotic insects at D1 and D3 (Superclusters S13 and S4), which presumably will help providing essential substrates for the imminent bacterial growth.[39] It is noteworthy that at D1 the insect is still fasting, suggesting that this provision of sugars and cofactors to the endosymbiont comes from larval reserves.

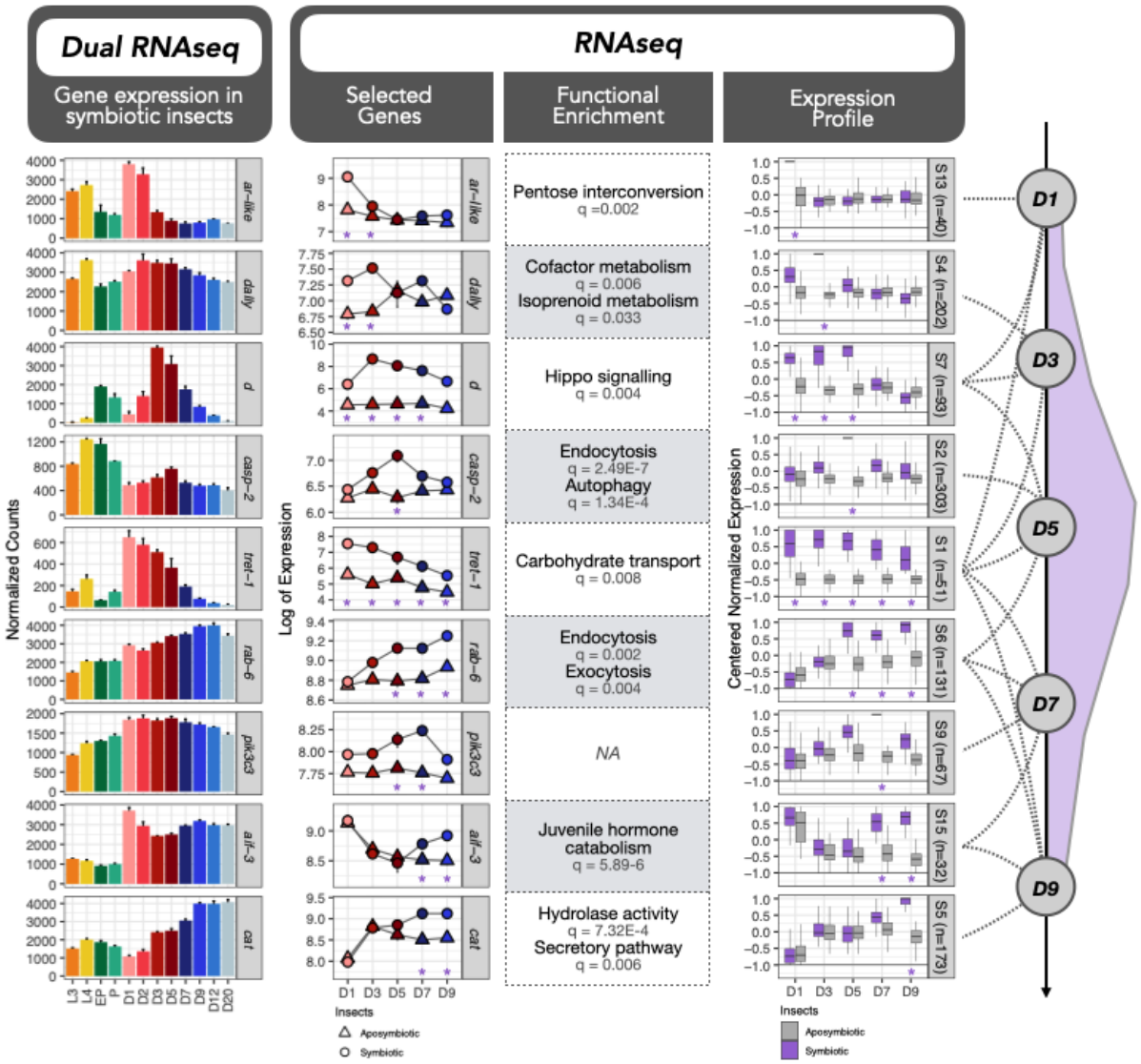

Figure 3. Clustering of genes differentially upregulated in symbiotic insects during the young adult bacterial dynamic. Expression profiles of selected genes are given for the dual RNA-seq and host RNA-seq datasets. Purple stars indicate in which stages we detected a significant up-regulation in symbiotic insects when compared to aposymbiotic within the RNAseq dataset. Functional enrichment of symbiotic superclusters provide functions specifically regulated in symbiotic weevils. On the far right, the bacterial load during the young adult development is shown in purple.

Host signaling pathways governing bacterial dynamics

Previous studies on endosymbiont maintenance and control indicated that chronic infection of intracellular bacteria in insects interferes with a broad range of cellular functions,[70] including oxidative stress,[71] immunity,[11,72] apoptosis and autophagy.[73,33] Nevertheless, little is known on the

regulatory and signaling pathways involved in bacterial load control while preserving host homeostasis.

In this view, we compiled all annotated genes from signaling pathways[39] differentially expressed either throughout the development of the cereal weevil or differentially expressed between symbiotic and aposymbiotic insects (Supplementary Table S17) in search for symbiotic-specific regulatory mechanisms. The strongest enrichment within signaling pathways was identified within the symbiotic/aposymbiotic RNA-seq dataset, regarding genes from the Hippo signaling pathway at D1, D3 and D5 (Supercluster S7, Figure 3). We found 43 genes (out of 49 homolog genes from this pathway in *Drosophila*), differentially expressed between symbiotic and aposymbiotic weevils, most of which were upregulated in symbiotic insects. In short, when the Hippo signaling pathway is inactivated, the transcriptional co-activator Yorkie (Yki) enters the nucleus and induces transcription of target genes, leading to growth (Figure 5A). When the Hippo signaling is activated, Warts kinase phosphorylates Yorkie, inducing its ubiquitination and degradation, therefore leading to a proliferation arrest. Hippo, Salvador (Sav), Kibra, Merlin (Mer) and Expanded (Ex) are examples of activators of the Hippo pathway, while Dachshous (Ds) and Dachs (D) are examples of repressors of Warts activity.

From both transcriptomic datasets (Figure 5B), we show that two repressors of Warts activity (*d* and *ds*) followed a symbiotic and time-dependent peak of expression at D3, and four activators of Hippo were induced in symbiotic insects either in a more stable manner up until D5 (*kibra*, *ex*) or with peak of expression precisely at D5 (*mer*, *sav*), suggesting a transcriptional activation of this pathway until D5, when the bacterial load climax is reached. Given that the regulation of this pathway relies heavily on post-transcriptional regulation (mostly phosphorylation and proteolysis) and that symbiotic and aposymbiotic weevils share the same genetic background as symbiotic ones, it is surprising to detect this activation of the Hippo signaling at the transcriptional level only in symbiotic weevils.

Moreover, the protein Ds is also involved in the non-canonical Wnt signaling pathway, which has already been hypothesized to play a role in weevil's bacteriocyte differentiation and bacteriome formation (Masson et al., 2015). Interestingly, a significant enrichment of "Regulation of Wnt receptor" was detected at the initial stages of adulthood (Supercluster SO65, Figure 2), with the presence of two copies of *dally* as previously mentioned. Besides *ds*, we found ten genes belonging to the Wnt signaling pathway that presented differential expression profiles, five of which (*mwh*, *daam*, *nmo* and two loci for *dally*) are induced in symbiotic weevils at D1 and D3

(Supercluster S4). Both Wnt and Hippo have been implicated in the growth regulation of disproportionally growing organs in the hemimetabolous cricket *Gryllus bimaculatus*.[74]

In sum, these results highlight specific regulatory factors from Hippo and Wnt pathways that might be central in the regulation of bacterial load in the cereal weevil. Nevertheless, further studies are needed to investigate whether these signaling pathways are regulating the increase in bacteriome size during the first days of adulthood, the bacterial load climax achieved around D5, or pre-signaling the following period of bacterial recycling and cell death.

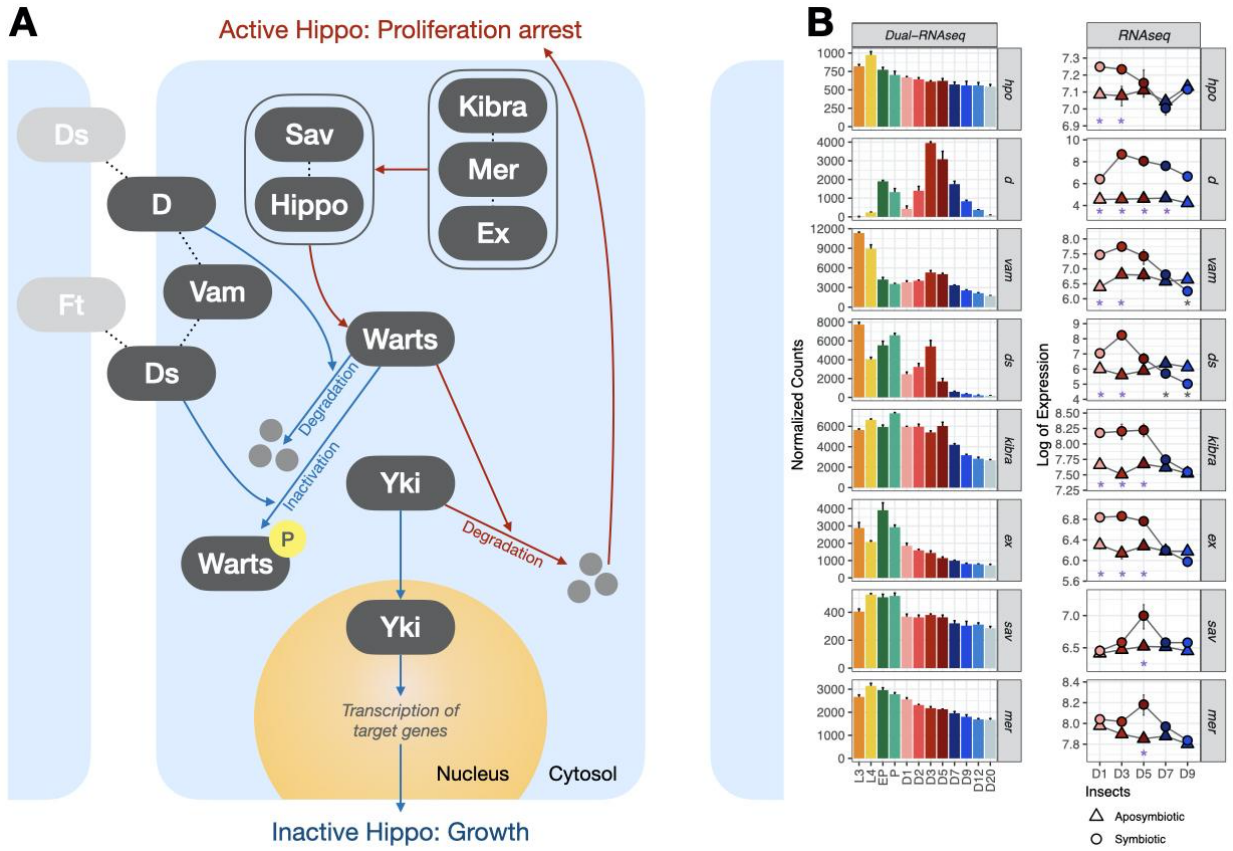

Figure 4. Hippo signaling in *S. oryzae*. A. Simplified diagram of the Hippo signaling pathway proposed in the cereal weevil B. Genes involved in Hippo signaling that were detected as differentially expressed throughout the life cycle of the cereal weevil (dual RNA-seq) and/or differentially expressed between symbiotic and aposymbiotic insects (RNA-seq). Stars indicate in which stages we detected a significant up-regulation (purple) or down-regulation (gray) in symbiotic insects when compared to aposymbiotic within the RNAseq dataset.

Nutritional immunity is central in the control of the endosymbiont load

Nutritional immunity, or the control over transition metals, is one of the first lines of defense against bacterial infections.[75] Iron, for example, is essential for all living organisms to transport oxygen and to produce energy. Nevertheless, since iron ions are capable of catalyzing destructive oxidative reactions, organisms have evolved various strategies for controlling and sequestering it.[76] Thus, bacteria have evolved parallel pathways to recover iron from different sources when starved for iron.[77] We have identified genes related to the sequestration of transition metal ions with profiles that showed an inverted (Supercluster SO41, Figure 2), or direct correlation with the bacterial load (Supercluster SO45 and SO70, Figure 2).

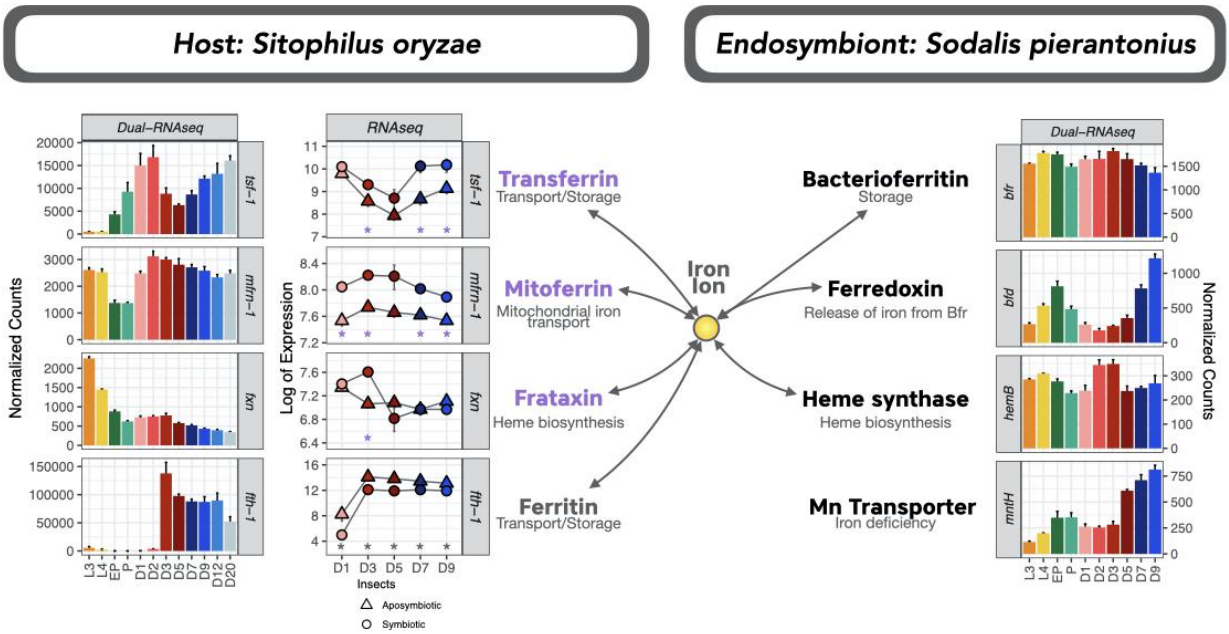

Figure 5. Expression of selected genes from iron metabolism in *S. oryzae* and *S. pierantonius* throughout the life cycle of the cereal weevil (dual RNA-seq) and/or differentially expressed between symbiotic and aposymbiotic insects (RNA-seq). Stars indicate in which stages we detected a significant up-regulation (purple) or down-regulation (gray) in symbiotic insects when compared to aposymbiotic within the RNAseq dataset.

In this respect, we have evaluated the expression profile of several genes involved in the metabolism, uptake and storage of metals from both insect and bacteria (Figure 4). As

differentially expressed between symbiotic and aposymbiotic insects we found genes encoding for Mitoferrin (*mfrn-1* gene, supercluster S7) and Frataxin (*fxn*, supercluster S4), two proteins involved in the mitochondrion iron metabolism. Moreover, both genes are highly expressed in larval bacteriome tissue within the dual RNA-seq data (Figure 4), strengthening the enrichment in expression within a symbiotic-specific tissue. Two proteins that can sequester iron and keep it from a destructive association with oxygen are transferrins (Tsf1) and ferritins (Ft).[76] Within the dual RNA-seq data, these proteins showed divergent transcriptomic profiles: while transferrin (*tsf-1*) had a profile similar to the inverted bacterial load (supercluster SO41), ferritin heavy chain-like (*fth-1*) expression peaked at D3 (supercluster SO45). Accordingly, in *Drosophila melanogaster*, these two proteins compete for iron in the intestine and also have an inverted balance (Law, 2002). The expression of both encoding genes was significantly different in symbiotic and aposymbiotic weevils: *tsf-1* had an overall higher expression in symbiotic insects, peaking at D1 and then again D7/D9, while *fth-1* had a higher expression in aposymbiotic insects (peaking at D3, Figure 4). In *Asobara tabida*, a parasitoid wasp in the family Braconidae, Kremer et al. (2009)[78] also showed that both heavy and light chains of ferritin were over-expressed in aposymbiotic insects. Transferrin, in turn, might be necessary in symbiotic insects either to sequester iron and limit its availability as a means to control bacterial growth, or to directly deliver iron to the endosymbiont. The first hypothesis has been proposed as a response mechanism to pathogenic bacteria in *D. melanogaster*,[79] while the latter was shown to take part in the homeostasis between *D. melanogaster* and *Spiroplasma poulsonii*.[80] On the other hand, aposymbiotic insects would need more ferritin to deal with iron excess (especially after emergence), or to transport it to other tissues. Moreover, the balance between both genes is important for the regulation of ferroptosis, an iron-dependent non-apoptotic cell death.[81]

Remarkably, we found a coordinated bacterial gene expression of iron-related proteins: a bacterioferritin-associated ferredoxin (*bfd*), with a profile similar to *tsf-1* (belonging to supercluster SP19), and a bacterioferritin (*bfrA*) with a slight peak around D3 (supercluster SP17), but globally highly expressed throughout the weevil's life cycle. In *Pseudomonas aeruginosa*, iron starvation downregulates *bfrA* while strongly upregulates *bfd* and vice-versa [82,83,84] Thus, the coordinated expression of such proteins in *S. pierantonius* indicates that at D2/D3 iron is highly available for the bacteria, which drastically decreases until D9. This is particularly supported by the expression of several heme biosynthetic genes, which peak from D1 to D3/D5 (Supercluster SP16, Figure 2; *hemB* in Figure 4). We believe the bacteria sense this decrease in iron content from D5 onwards. Knowing that other metals can occasionally substitute iron in activating at least some

metalloenzymes, we looked at the expression of other metal related genes, and found that the manganese transporter *mntH* (Figure 4), which can support the growth of iron-deprived bacteria,[85] was highly upregulated from D5 to D9 (supercluster SP4). Interestingly, we also detected an increase in the expression of a Zinc uptake gene (*zntB*) from D1 to D3, which has been associated with nutritional immunity.[86]

Host recycling genes and bacterial stress response anticipate active bacterial clearance

We have previously shown that endosymbiont clearance and recycling involves bacteriocyte autophagy and apoptosis (Vigneron et al., 2014). Even though the transcription of the autophagy factor *atg6* has been detected prior to active bacterial recycling,[87] our initial hypothesis was that the accumulation of DOPA at D6 triggered apoptosis. More recently, we pinpointed that DOPA increase was concomitant with the endosymbiont clearance rather than anticipating it.[34] In accordance with Dell'Aglio et al. (2023), we detected here a strong enrichment of autophagy and endosomal transport starting at D5 (supercluster SO70, Figure 2), before the active endosymbiont clearance. Moreover, all superclusters presenting a functional enrichment in autophagy (SO29, SO31, and SO39, Figure 2) had the lowest expression at D1 and D2, indicating the inhibition of autophagic genes at these early stages, and a gradual increase starting at D3. Finally, other cell-death and immune related genes, belonging to enriched functions such as exocytosis, immune effector process and response to bacterium increase gradually from D5 to D20 (superclusters SO39 and SO69 from Figure 2). One example is the gene coding for the antimicrobial peptide Acanthoscurrin-2 (*acn-2*, supercluster SO69), which showed a prominent increase in expression of around 200 fold between D1 and D20.

The enrichment of endocytosis and autophagy at D5 and exocytosis and immune effectors (specified with the GO term antigen processing and presentation) at D5, D7, and D9 were further confirmed as symbiotic-specific processes (Superclusters S2 and S6, Figure 3). Hydrolase activity, essential for the final recycling of bacterial cell debris, is enriched specifically in symbiotic weevils at D9 (Supercluster S5). Nevertheless, the complex equilibrium between pro-apoptotic and pro-survival factors varies throughout the life cycle of the cereal weevil. Thus, the complex and symbiotic-specific expression of the Hippo signaling pathway, along with components from the Wnt pathway, possibly play a role in the regulation of programmed cell death of bacteriocytes (Figure 6).

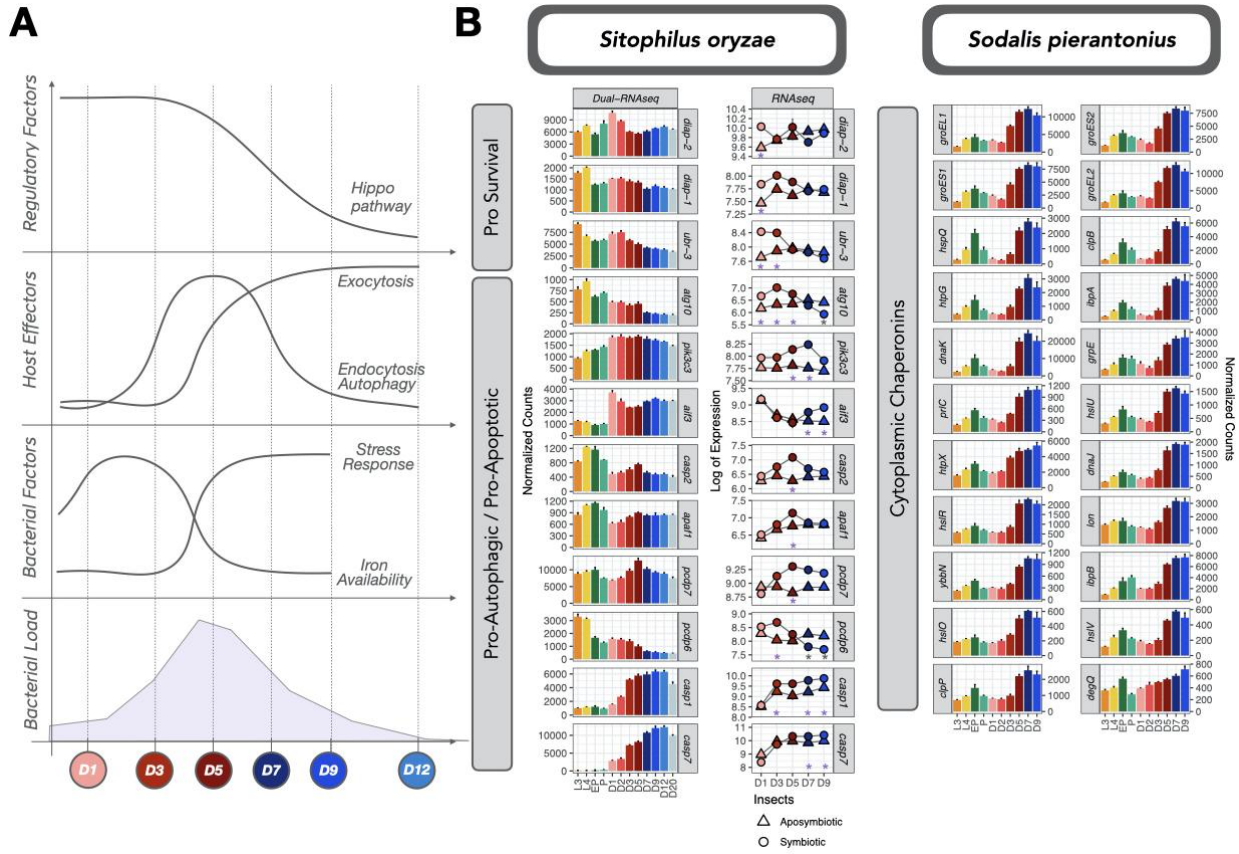

Figure 6. Insect and bacterial factors involved in the clearance of bacteria. (A) Schematic profiles of expression of host regulatory pathway Hippo, host effectors involved in exocytosis, endocytosis and autophagy as well as bacterial stress response genes depict a complex but coordinated regulation between both symbiotic partners. We also included the bacterial perceived iron availability (as predicted by the expression of iron sensing genes from Figure 5). (B) Selection of deregulated pro-survival pro-apoptotic / pro-autophagic genes from the cereal weevil as well as all cytoplasmic chaperonins involved in stress response from the endosymbiont throughout the life cycle of the cereal weevil (dual RNA-seq) and/or differentially expressed between symbiotic and aposymbiotic insects (RNA-seq). Stars indicate in which stages we detected a significant up-regulation (purple) or down-regulation (gray) in symbiotic insects when compared to aposymbiotic within the RNAseq dataset.

While most effectors of cell death were induced in symbiotic insects at D5 and later, some presented a significant up-regulation at D3, such as *atg-10* and *pdcd-6*. Pro-survival genes *diap-1*, *diap-2* and *ubr-3* were highly expressed at the initial stages of adulthood and were sharply downregulated at D5. The protein Ubr3 is known to regulate the activity of Diap1 in *Drosophila*,[88] and its knockout was shown to induce caspase-dependent apoptosis. Accordingly, executioner caspases (*casp-1*, *casp-2* and *casp-7*) were all upregulated in symbiotic insects at D5. Even though no initiator caspase has been identified in the cereal weevil so far, the gene responsible for the activation of such a caspase was also highly induced at D5 (*apaf-1*). Interestingly, increased levels of caspases in *Drosophila* were detected with the knockdown of the *fth-1*

homolog.[89] Here, we show lower levels of *fth-1* along with increased levels of caspases in symbiotic insects when compared to aposymbiotics. In sum, apoptosis is likely functional as early as D5, with the induction of pro-apoptotic and pro-autophagic genes and depletion of pro-survival ones. At D3, even though the expression of some genes involved in programmed cell-death and autophagy is observed, pro-survival effectors most likely balance out the apoptotic effects, in accordance with our previous studies that show no distinct sign of apoptosis of bacteriocytes at D3 (Vigneron et al., 2014).

Ubiquitination-related processes, which have been extensively involved in the induction of both apoptosis and autophagy, especially in host-bacterial interactions,[90] were also enriched at D5 (both in the dual RNA-seq data, superclusters SO70 and SO76, and between symbiotic and aposymbiotic weevils, supercluster S2). As previously mentioned, the genome of *S. pierantonius* bears a single deubiquitinase *sseL*, which is known to inhibit autophagic clearance of cytoplasmic aggregates of *Salmonella*.[60] This gene is induced at N, D1 and D2 stages in *S. pierantonius*, and this regulation decreases from D3 onwards. This suggests that, if the deubiquitinase SseL acts similarly in *S. pierantonius*, the bacteria could be actively helping the inhibition of apoptosis within the host at the early days of adulthood.

Finally, we identified a major increase in expression of cytoplasmic chaperonins in the bacteria at D5, D7 and D9 (Figure 6, superclusters SP4, SP19 and SP23 from Figure 2, SP6, SP17 from Supplementary Figure S6). This enrichment in stress response genes is indeed the most significant enrichment within all bacterial clusters. Most chaperonins also have smaller peaks of expression at EP stage (Figure 6), during the period that endosymbionts exit bacteriomes and infect stem cells during metamorphosis, and thus are no longer protected from the immune system within bacteriocytes. In line with the fact that endocytosis, apoptosis, autophagy and other stress signals are activated prior to the active recycling of bacteria, some of these chaperones were already induced at D3, including the chaperonins *groEL* and *groES*. In weevils, GroEL has been previously described to have a central role in the inhibition of *S. pierantonius* division, through the interaction with ColA peptide.[56] The gene *ychH*, which codes for a putative inner membrane stress-induced protein, presented a similar profile. Interestingly, this gene was detected as the most repressed gene of *D. dadantii* during *A. pisum* infection.[53]

Despite this massive activation of stress genes, the general sigma factor responsible for the stress response *rpoH* did not present the same profile (supercluster SP2). A transcriptional regulator involved in stress that follows the overall pattern of expression of the aforementioned chaperones

(supercluster SP28 from Supplementary Figure S6), but which nonetheless has never been shown to regulate any of them, codes for the cell division protein BolA. The molecular mechanisms allowing a bacterial response to external signals are extremely complex and often involve two-component transduction systems (TCSs). Interestingly, *ompR*, a response regulator of the TCS pathway, which senses acid pH and osmotic stress, is also highly induced at D5 to D9 in *S. pierantonius* (supercluster SP4). This particular gene regulates the expression of virulence related genes in *Salmonella*,[91,92] *Yersinia*,[93,94] and *Shigella*.[95] The bacteria are presumably sensing an acidic pH within the host autophagic vesicles and by D5, most tRNAs are downregulated (Supplementary Figure S12), indicating a general and abrupt bacterial translational arrest.

Conclusions

The trade-off between host benefit and endosymbiont burden is central to the understanding of symbiosis establishment and maintenance. Whereas endosymbiont dynamics and load changes have been reported in several model systems, very little is known on genes and cellular pathways associated with host-symbiont trade-off. In this study, we performed a comprehensive transcriptomic approach that includes dual RNA-seq and RNA-seq on symbiotic and aposymbiotic insects, to identify key functions in both insect and bacteria acting on bacterial dynamics at key development stages of cereals weevils (Figure 6).

We showed that at the last larval stages, both bacteria and host activate cellular and metabolic processes, which may help anticipate the morphological changes occurring during metamorphosis, and store energy reserves before a fasting period begins. During metamorphosis, endosymbionts exit bacteriocytes and infect midgut stem cells that differentiate latter into new bacteriocytes.[29] Whether or not the concomitant increase in AMP expression at the pupal stage is the host response to the bacterial behavior outside the bacteriocyte remains still a puzzling question. We also pinpointed out a novel putative intracellular AMP, coding for a partial Diptericin-like (*dpt-like partial*), highly correlated with bacterial load and likely to be involved in endosymbiont control.

The massive differential expression between symbiotic and aposymbiotic adults showed that endosymbiont presence greatly affects the gene expression within weevils. Regarding the contrasted bacterial dynamics, we examined the regulatory mechanisms involved in endosymbiont proliferation, bacterial load climax and recycling. Symbiotic adults showed a

massive enrichment in functions related to carbohydrate metabolism, in agreement with our previous work demonstrating that endosymbiont proliferation relies solely on the availability of carbohydrates from diet intake.[34] Nevertheless, we highlighted biological functions intertwined and coregulated, including the Hippo signaling pathway, likely governing bacterial dynamics, and bacterial cellular stress at the onset of endosymbiont recycling. Nutritional immunity through iron availability was shown to be central for the control of bacterial load climax, and has been linked with both the Hippo signaling and apoptosis in *Drosophila*.[89,96]

Even though early signals of apoptosis and autophagy were detected early on (D3), apoptosis is molecularly functional from D5 onwards, with both the induction of pro-apoptotic and pro-autophagic genes and the depletion of pro-survival ones from both bacteria and insect. As the molecular recycling process begins, the bacteria sense this stress and activate a global stress response along with a massive translational arrest from D5 to D9. Following the bacterial recycling at D12/D20, we no longer detect changes in expression within the insect, which suggests that cell homeostasis within the gut is restored.

Future perspectives of this work include the integration with a reconstructed genome-wide metabolic network from both insect and bacterium, in order to gain insights into complete metabolic pathways. The complete study of these tightly regulated metabolic functions, which are at the center of symbiotic exchanges, will help to understand how the host and bacteria finely tune their gene expression and respond to physiological challenges constrained by insect development in a nutritionally limited ecological niche.

Acknowledgments

This work was funded by the ANR GREEN (ANR-17-CE20-0031-01 - A. Heddi) and ANR UNLEASh (ANR UNLEASH-CE20-0015-01 - R. Rebollo). This work was performed using the computing facilities of the CC LBBE/PRABI. Dual RNA-seq library construction and sequencing was performed at the sequencing platform of the Institut de Génomique Fonctionnelle de Lyon, Ecole Normale Supérieure de Lyon, France. Sequencing for the RNA-seq library was performed by the GenomEast platform, a member of the 'France Génomique' consortium (ANR-10-INBS-0009). The authors wish to thank the DTAMB platform and Jihane Mennana for technical help regarding quantitative PCRs.

Data and Code Availability

Raw sequencing data from this study have been deposited at the National Center for Biotechnology Information (NCBI) Sequence Read Archive (SRA) under PRJNA918957.

This article does not report original code.

Author Contributions

AH, NP and RR conceived the original project. AV was responsible for all the molecular biology methods, with the help of EDA and OH. AV in collaboration with SH and BG constructed the dual RNA-seq libraries and produced the sequencing reads. AV constructed the RNA-seq libraries and produced the sequencing reads. MGF was responsible for the bioinformatic analyses of the dual RNA-seq and RNA-seq. MGF analyzed the data with the help of NP, RR, GC, and AH. MGF, AH, NP and RR wrote the manuscript with the help of CVM, GC and AZR. All authors read and approved the final manuscript.

Declaration of interests

The authors declare no competing interests.

Supplemental information

Figures

S1: Bioinformatics methodology for dual RNA-seq

S2: Euclidean clustering of sequencing samples

S3: PCA Clustering of sequencing samples

S4: Bacterial reads from dual RNA-seq

S5: Profile of dual RNA-seq superclusters from *Sitophilus oryzae*

S6: Profile of dual RNA-seq superclusters from *Sodalis pierantonius*

S7: Detailed analysis of putative deubiquitinase SseL

S8: Expression profiles of selected antimicrobial peptides from *Sitophilus oryzae*

S9: Upsettr plot from RNA-seq data between symbiotic and aposymbiotic *Sitophilus oryzae*

S10: Profile of RNA-seq superclusters from symbiotic *Sitophilus oryzae*

S11: Profile of RNA-seq superclusters from aposymbiotic *Sitophilus oryzae*

S12: tRNA expression profiles from *Sodalis pierantonius*

Tables

S1: Dual RNA-seq mapping statistics

S2: Dual RNA-seq gene counts from *Sitophilus oryzae*

S3: Dual RNA-seq gene counts from *Sodalis pierantonius*

S4: Dual RNA-seq DEG from *Sitophilus oryzae*

S5: Dual RNA-seq DEG from *Sodalis pierantonius*

S6: Dual RNA-seq LRT results from *Sitophilus oryzae*

S7: Dual RNA-seq LRT results from *Sodalis pierantonius*

S8: RNA-seq gene counts from symbiotic and aposymbiotic *Sitophilus oryzae*

S9: RNA-seq DEG from symbiotic and aposymbiotic *Sitophilus oryzae*

S10: Profile of dual RNA-seq superclusters from *Sitophilus oryzae*

S11: Profile of dual RNA-seq superclusters from *Sodalis pierantonius*

S12: Profile of RNA-seq superclusters from symbiotic and aposymbiotic *Sitophilus oryzae*

S13: Dual RNA-seq functional enrichment analysis of supercluster from *Sitophilus oryzae*

S14: Dual RNA-seq functional enrichment analysis of supercluster from *Sodalis pierantonius*

S15: RNA-seq functional enrichment analysis of supercluster from symbiotic and aposymbiotic *Sitophilus oryzae*

S16: List of genes and abbreviations within main text

S17: List of signaling and immunity genes

References

1. Douglas, A.E. (1998). Nutritional interactions in insect-microbial symbioses: aphids and their symbiotic bacteria Buchnera. Annu. Rev. Entomol. *43*. 10.1146/annurev.ento.43.1.17.

2. Moya, A., Peretó, J., Gil, R., and Latorre, A. (2008). Learning how to live together: genomic insights into prokaryote-animal symbioses. Nat. Rev. Genet. *9*. 10.1038/nrg2319.

3. Nyholm, S.V., Stewart, J.J., Ruby, E.G., and McFall-Ngai, M.J. (2009). Recognition between symbiotic Vibrio fischeri and the haemocytes of Euprymna scolopes. Environ. Microbiol. *11*. 10.1111/j.1462-2920.2008.01788.x.

4. Tsuchida, T., Koga, R., Horikawa, M., Tsunoda, T., Maoka, T., Matsumoto, S., Simon, J.C., and Fukatsu, T. (2010). Symbiotic bacterium modifies aphid body color. Science *330*. 10.1126/science.1195463.

5. Troll, J.V., Bent, E.H., Pacquette, N., Wier, A.M., Goldman, W.E., Silverman, N., and McFall-Ngai, M.J. (2010). Taming the symbiont for coexistence: a host PGRP neutralizes a bacterial symbiont toxin. Environ. Microbiol. *12*. 10.1111/j.1462-2920.2009.02121.x.

6. McCutcheon, J.P., and Moran, N.A. (2011). Extreme genome reduction in symbiotic bacteria. Nat. Rev. Microbiol. *10*. 10.1038/nrmicro2670.

7. Weiss, M., Sýkorová, Z., Garnica, S., Riess, K., Martos, F., Krause, C., Oberwinkler, F., Bauer, R., and Redecker, D. (2011). Sebacinales everywhere: previously overlooked ubiquitous fungal endophytes. PLoS One *6*. 10.1371/journal.pone.0016793.

8. Martinez, A.J., Weldon, S.R., and Oliver, K.M. (2014). Effects of parasitism on aphid nutritional and protective symbioses. Mol. Ecol. *23*. 10.1111/mec.12550.

9. Flórez, L.V., Biedermann, P.H., Engl, T., and Kaltenpoth, M. (2015). Defensive symbioses of animals with prokaryotic and eukaryotic microorganisms. Nat. Prod. Rep. *32*. 10.1039/c5np00010f.

10. Masson, F., Zaidman-Rémy, A., and Heddi, A. (2016). Antimicrobial peptides and cell processes tracking endosymbiont dynamics. Philos. Trans. R. Soc. Lond. B Biol. Sci. *371*. 10.1098/rstb.2015.0298.

11. Maire, J., Vincent-Monégat, C., Masson, F., Zaidman-Rémy, A., and Heddi, A. (2018). An IMD-like pathway mediates both endosymbiont control and host immunity in the cereal weevil Sitophilus spp. Microbiome *6*. 10.1186/s40168-017-0397-9.

12. Douglas, A.E. (2020). Housing microbial symbionts: evolutionary origins and diversification of symbiotic organs in animals. Philos. Trans. R. Soc. Lond. B Biol. Sci. *375*. 10.1098/rstb.2019.0603.

13. Ferrarini, M.G., Dell'Aglio, E., Vallier, A., Balmand, S., Vincent-Monégat, C., Hughes, S., Gillet, B., Parisot, N., Zaidman-Rémy, A., Vieira, C., et al. (2022). Efficient compartmentalization in insect bacteriomes protects symbiotic bacteria from host immune system. Microbiome *10*. 10.1186/s40168-022-01334-8.

14. Moran, N.A. (1996). Accelerated evolution and Muller's rachet in endosymbiotic bacteria. Proc. Natl. Acad. Sci. U. S. A. *93*. 10.1073/pnas.93.7.2873.

15. Wernegreen, J.J., and Moran, N.A. (1999). Evidence for genetic drift in endosymbionts (Buchnera): analyses of protein-coding genes. Mol. Biol. Evol. *16*. 10.1093/oxfordjournals.molbev.a026040.

16. Gil, R., Belda, E., Gosalbes, M.J., Delaye, L., Vallier, A., Vincent-Monégat, C., Heddi, A., Silva, F.J., Moya, A., and Latorre, A. (2008). Massive presence of insertion sequences in the genome of SOPE, the primary endosymbiont of the rice weevil Sitophilus oryzae. Int. Microbiol. *11*.

17. Burke, G.R., and Moran, N.A. (2011). Massive genomic decay in Serratia symbiotica, a recently evolved symbiont of aphids. Genome Biol. Evol. *3*. 10.1093/gbe/evr002.

18. Gillespie, J.J., Joardar, V., Williams, K.P., Driscoll, T., Hostetler, J.B., Nordberg, E., Shukla, M., Walenz, B., Hill, C.A., Nene, V.M., et al. (2012). A Rickettsia Genome Overrun by Mobile Genetic Elements Provides Insight into the Acquisition of Genes Characteristic of an Obligate Intracellular Lifestyle. J. Bacteriol. *194*, 376. 10.1128/JB.06244-11.

19. Oakeson, K.F., Gil, R., Clayton, A.L., Dunn, D.M., von Niederhausern, A.C., Hamil, C., Aoyagi, A., Duval, B., Baca, A., Silva, F.J., et al. (2014). Genome degeneration and adaptation in a nascent stage of symbiosis. Genome Biol. Evol. *6*. 10.1093/gbe/evt210.

20. Latorre, A., and Manzano-Marín, A. (2017). Dissecting genome reduction and trait loss in insect endosymbionts. Ann. N. Y. Acad. Sci. *1389*. 10.1111/nyas.13222.

21. Shigenobu, S., Watanabe, H., Hattori, M., Sakaki, Y., and Ishikawa, H. (2000). Genome sequence of the endocellular bacterial symbiont of aphids Buchnera sp. APS. Nature *407*. 10.1038/35024074.

22. Dale, C., Young, S.A., Haydon, D.T., and Welburn, S.C. (2001). The insect endosymbiont Sodalis glossinidius utilizes a type III secretion system for cell invasion. Proc. Natl. Acad. Sci. U. S. A. *98*. 10.1073/pnas.98.4.1883.

23. Moran, N.A., and Mira, A. (2001). The process of genome shrinkage in the obligate symbiont Buchnera aphidicola. Genome Biol. *2*. 10.1186/gb-2001-2-12-research0054.

24. Reymond, N., Calevro, F., Viñuelas, J., Morin, N., Rahbé, Y., Febvay, G., Laugier, C., Douglas, A., Fayard, J.M., and Charles, H. (2006). Different levels of transcriptional regulation due to trophic constraints in the reduced genome of Buchnera aphidicola APS. Appl. Environ. Microbiol. *72*. 10.1128/AEM.01118-06.

25. Gerardo, N.M., Altincicek, B., Anselme, C., Atamian, H., Barribeau, S.M., de Vos, M., Duncan, E.J., Evans, J.D., Gabaldón, T., Ghanim, M., et al. (2010). Immunity and other defenses in pea aphids, Acyrthosiphon pisum. Genome Biol. *11*. 10.1186/gb-2010-11-2-r21.

26. Shigenobu, S., and Wilson, A.C. (2011). Genomic revelations of a mutualism: the pea aphid and its obligate bacterial symbiont. Cell. Mol. Life Sci. *68*. 10.1007/s00018-011-0645-2.

27. Hansen, A.K., and Moran, N.A. (2011). Aphid genome expression reveals host-symbiont

cooperation in the production of amino acids. Proc. Natl. Acad. Sci. U. S. A. *108*. 10.1073/pnas.1013465108.

28. Clayton, A.L., Oakeson, K.F., Gutin, M., Pontes, A., Dunn, D.M., von Niederhausern, A.C., Weiss, R.B., Fisher, M., and Dale, C. (2012). A Novel Human-Infection-Derived Bacterium Provides Insights into the Evolutionary Origins of Mutualistic Insect–Bacterial Symbioses. PLoS Genet. *8*. 10.1371/journal.pgen.1002990.

29. Maire, J., Parisot, N., Ferrarini, M.G., Vallier, A., Gillet, B., Hughes, S., Balmand, S., Vincent-Monégat, C., Zaidman-Rémy, A., and Heddi, A. (2020). Spatial and morphological reorganization of endosymbiosis during metamorphosis accommodates adult metabolic requirements in a weevil. Proc. Natl. Acad. Sci. U. S. A. *117*, 19347. 10.1073/pnas.2007151117.

30. Maire, J., Vincent-Monégat, C., Balmand, S., Vallier, A., Hervé, M., Masson, F., Parisot, N., Vigneron, A., Anselme, C., Perrin, J., et al. (2019). Weevil pgrp-lb prevents endosymbiont TCT dissemination and chronic host systemic immune activation. Proc. Natl. Acad. Sci. U. S. A. *116*. 10.1073/pnas.1821806116.

31. Werren, J.H., Baldo, L., and Clark, M.E. (2008). Wolbachia: master manipulators of invertebrate biology. Nat. Rev. Microbiol. *6*. 10.1038/nrmicro1969.

32. Nardon, P. (1973). Obtention d'une souche asymbiotique chez le charan\ccon Sitophilus sasakii: Diff'erentes m'ethodes et comparaison avec la souche symbiotique d'origine. CR Acad Sci Paris D *3*, 65–67.

33. Vigneron, A., Masson, F., Vallier, A., Balmand, S., Rey, M., Vincent-Monégat, C., Aksoy, E., Aubailly-Giraud, E., Zaidman-Rémy, A., and Heddi, A. (2014). Insects recycle endosymbionts when the benefit is over. Curr. Biol. *24*. 10.1016/j.cub.2014.07.065.

34. Dell'Aglio, E., Lacotte, V., Peignier, S., Rahioui, I., Benzaoui, F., Vallier, A., Da Silva, P., Desouhant, E., Heddi, A., and Rebollo, R. (2023). Weevil Carbohydrate Intake Triggers Endosymbiont Proliferation: A Trade-Off between Host Benefit and Endosymbiont Burden. MBio. 10.1128/mbio.03333-22.

35. Martin, M. (2011). Cutadapt removes adapter sequences from high-throughput sequencing reads. EMBnet J. *17*, 10. 10.14806/ej.17.1.200.

36. Dobin, A., Davis, C.A., Schlesinger, F., Drenkow, J., Zaleski, C., Jha, S., Batut, P., Chaisson, M., and Gingeras, T.R. (2013). STAR: ultrafast universal RNA-seq aligner. Bioinformatics *29*. 10.1093/bioinformatics/bts635.

37. Langmead, B., and Salzberg, S.L. (2012). Fast gapped-read alignment with Bowtie 2. Nat. Methods *9*. 10.1038/nmeth.1923.

38. Li, H., Handsaker, B., Wysoker, A., Fennell, T., Ruan, J., Homer, N., Marth, G., Abecasis, G., and Durbin, R. (2009). The Sequence Alignment/Map format and SAMtools. Bioinformatics *25*. 10.1093/bioinformatics/btp352.

39. Parisot, N., Vargas-Chávez, C., Goubert, C., Baa-Puyoulet, P., Balmand, S., Beranger, L., Blanc, C., Bonnamour, A., Boulesteix, M., Burlet, N., et al. (2021). The transposable element-rich genome of the cereal pest Sitophilus oryzae. BMC Biol. *19*. 10.1186/s12915-

021-01158-2.

40. Liao, Y., Smyth, G.K., and Shi, W. (2014). featureCounts: an efficient general purpose program for assigning sequence reads to genomic features. Bioinformatics *30*. 10.1093/bioinformatics/btt656.

41. Varet, H., Brillet-Guéguen, L., Coppée, J.Y., and Dillies, M.A. (2016). SARTools: A DESeq2- and EdgeR-Based R Pipeline for Comprehensive Differential Analysis of RNA-Seq Data. PLoS One *11*. 10.1371/journal.pone.0157022.

42. Love, M.I., Huber, W., and Anders, S. (2014). Moderated estimation of fold change and dispersion for RNA-seq data with DESeq2. Genome Biol. *15*. 10.1186/s13059-014-0550-8.

43. Benjamini, Y., and Hochberg, Y. (1995). Controlling the false discovery rate: A practical and powerful approach to multiple testing. J. R. Stat. Soc. *57*, 289–300. 10.1111/j.2517-6161.1995.tb02031.x.

44. Kiddle, S.J., Windram, O.P., McHattie, S., Mead, A., Beynon, J., Buchanan-Wollaston, V., Denby, K.J., and Mukherjee, S. (2010). Temporal clustering by affinity propagation reveals transcriptional modules in Arabidopsis thaliana. Bioinformatics *26*. 10.1093/bioinformatics/btp673.

45. R Core Team R Foundation for Statistical Computing R: A Language and Environment for Statistical Computing. CRAN.

46. Kolde, R. (2019). pheatmap: Pretty Heatmaps.

47. Wickham, H. (2016). ggplot2: Elegant Graphics for Data Analysis (Springer-Verlag New York, 2016).

48. Wu, T., Hu, E., Xu, S., Chen, M., Guo, P., Dai, Z., Feng, T., Zhou, L., Tang, W., Zhan, L., et al. (2021). clusterProfiler 4.0: A universal enrichment tool for interpreting omics data. Innovation (Camb) *2*, 100141. 10.1016/j.xinn.2021.100141.

49. Ashburner, M., Ball, C.A., Blake, J.A., Botstein, D., Butler, H., Cherry, J.M., Davis, A.P., Dolinski, K., Dwight, S.S., Eppig, J.T., et al. (2000). Gene ontology: tool for the unification of biology. The Gene Ontology Consortium. Nat. Genet. *25*, 25–29. 10.1038/75556.

50. Kanehisa, M., and Goto, S. (2000). KEGG: kyoto encyclopedia of genes and genomes. Nucleic Acids Res. *28*, 27–30. 10.1093/nar/28.1.27.

51. Supek, F., Bošnjak, M., Škunca, N., and Šmuc, T. (2011). REVIGO summarizes and visualizes long lists of gene ontology terms. PLoS One *6*. 10.1371/journal.pone.0021800.

52. Zhang, H., Stallock, J.P., Ng, J.C., Reinhard, C., and Neufeld, T.P. (2000). Regulation of cellular growth by the Drosophila target of rapamycin dTOR. Genes Dev. *14*. 10.1101/gad.835000.

53. Costechareyre, D., Chich, J.-F., Strub, J.-M., Rahbé, Y., and Condemine, G. (2013). Transcriptome of Dickeya dadantii infecting Acyrthosiphon pisum reveals a strong defense against antimicrobial peptides. PLoS One *8*, e54118. 10.1371/journal.pone.0054118.

54. Clayton, A.L., Enomoto, S., Su, Y., and Dale, C. (2017). The Regulation of Antimicrobial Peptide Resistance in the Transition to Insect Symbiosis. Mol. Microbiol. *103*, 958. 10.1111/mmi.13598.

55. Pontes, M.H., Smith, K.L., De Vooght, L., Den Abbeele J, V., and Dale, C. (2011). Attenuation of the sensing capabilities of PhoQ in transition to obligate insect-bacterial association. PLoS Genet. *7*. 10.1371/journal.pgen.1002349.

56. Login, F.H., Balmand, S., Vallier, A., Vincent-Monégat, C., Vigneron, A., Weiss-Gayet, M., Rochat, D., and Heddi, A. (2011). Antimicrobial peptides keep insect endosymbionts under control. Science *334*. 10.1126/science.1209728.

57. Heddi, A., Lefebvre, F., and Nardon, P. (1993). Effect of endocytobiotic bacteria on mitochondrial enzymatic activities in the weevil Sitophilus oryzae (Coleoptera : Curculionidae). Insect Biochem. Mol. Biol. *23*, 403–411. 10.1016/0965-1748(93)90024-m.

58. Heddi, A., Grenier, A.M., Khatchadourian, C., Charles, H., and Nardon, P. (1999). Four intracellular genomes direct weevil biology: nuclear, mitochondrial, principal endosymbiont, and Wolbachia. Proc. Natl. Acad. Sci. U. S. A. *96*. 10.1073/pnas.96.12.6814.

59. Jennings, E., Thurston, T.L.M., and Holden, D.W. (2017). Salmonella SPI-2 Type III Secretion System Effectors: Molecular Mechanisms And Physiological Consequences. Cell Host Microbe *22*, 217–231. 10.1016/j.chom.2017.07.009.

60. Mesquita, F.S., Thomas, M., Sachse, M., Santos, A.J.M., Figueira, R., and Holden, D.W. (2012). The Salmonella deubiquitinase SseL inhibits selective autophagy of cytosolic aggregates. PLoS Pathog. *8*, e1002743. 10.1371/journal.ppat.1002743.

61. Hanson, M.A., and Lemaitre, B. (2020). New insights on Drosophila antimicrobial peptide function in host defense and beyond. Curr. Opin. Immunol. *62*. 10.1016/j.coi.2019.11.008.

62. Cociancich, S., Bulet, P., Hetru, C., and Hoffmann, J.A. (1994). The inducible antibacterial peptides of insects. Parasitol. Today *10*. 10.1016/0169-4758(94)90260-7.

63. Vasilchenko, A.S., and Rogozhin, E.A. (2019). Sub-inhibitory Effects of Antimicrobial Peptides. Front. Microbiol. *10*. 10.3389/fmicb.2019.01160.

64. Duperthuy, M. (2020). Antimicrobial Peptides: Virulence and Resistance Modulation in Gram-Negative Bacteria. Microorganisms *8*. 10.3390/microorganisms8020280.

65. Nardon, P., Grenier, A.M., and Heddi, A. (1998). Endocytobiote control by the host in the weevil Sitophilus oryzae, Coleoptera, Curculionidae. Symbiosis.

66. James, V., and Hugouvieux-Cotte-Pattat, N. (1996). Regulatory systems modulating the transcription of the pectinase genes of Erwinia chrysanthemi are conserved in Escherichia coli. Microbiology *142 (Pt 9)*. 10.1099/00221287-142-9-2613.

67. Rodionov, D.A., Mironov, A.A., Rakhmaninova, A.B., and Gelfand, M.S. (2000). Transcriptional regulation of transport and utilization systems for hexuronides, hexuronates and hexonates in gamma purple bacteria. Mol. Microbiol. *38*. 10.1046/j.1365-2958.2000.02115.x.

68. Nasser, W., Reverchon, S., Condemine, G., and Robert-Baudouy, J. (1994). Specific interactions of Erwinia chrysanthemi KdgR repressor with different operators of genes involved in pectinolysis. J. Mol. Biol. *236*. 10.1006/jmbi.1994.1155.

69. Ma, H., Zhao, H., Liu, F., Zhao, H., Kong, R., Shi, L., Wei, M., and Li, Z. (2019). Heparan sulfate negatively regulates intestinal stem cell proliferation in Drosophila adult midgut. Biol. Open *8*. 10.1242/bio.047126.

70. Ratzka, C., Gross, R., and Feldhaar, H. (2012). Endosymbiont Tolerance and Control within Insect Hosts. Insects *3*, 553. 10.3390/insects3020553.

71. Kremer, N., Charif, D., Henri, H., Gavory, F., Wincker, P., Mavingui, P., and Vavre, F. (2012). Influence of Wolbachia on host gene expression in an obligatory symbiosis. BMC Microbiol. *12 Suppl 1*. 10.1186/1471-2180-12-S1-S7.

72. Ferrarini, M.G., Vallier, A., Dell'Aglio, E., Balmand, S., Vincent-Monégat, C., Debbache, M., Maire, J., Parisot, N., Zaidman-Rémy, A., Heddi, A., et al. (2023). Endosymbiont-containing germarium transcriptional survey in a cereal weevil depicts downregulation of immune effectors at the onset of sexual maturity. Front. Physiol. *14*. 10.3389/fphys.2023.1142513.

73. Vigneron, A., Charif, D., Vincent-Monégat, C., Vallier, A., Gavory, F., Wincker, P., and Heddi, A. (2012). Host gene response to endosymbiont and pathogen in the cereal weevil Sitophilus oryzae. BMC Microbiol. *12 Suppl 1*. 10.1186/1471-2180-12-S1-S14.

74. Ohde, T., Mito, T., and Niimi, T. (2022). A hemimetabolous wing development suggests the wing origin from lateral tergum of a wingless ancestor. Nat. Commun. *13*. 10.1038/s41467-022-28624-x.

75. Iatsenko, I., Marra, A., Boquete, J.P., Peña, J., and Lemaitre, B. (2020). Iron sequestration by transferrin 1 mediates nutritional immunity in Drosophila melanogaster. Proc. Natl. Acad. Sci. U. S. A. *117*. 10.1073/pnas.1914830117.

76. Gorman, M.J. (2023). Iron Homeostasis in Insects. Annu. Rev. Entomol. *68*, 51–67. 10.1146/annurev-ento-040622-092836.

77. Parrow, N.L., Fleming, R.E., and Minnick, M.F. (2013). Sequestration and scavenging of iron in infection. Infect. Immun. *81*, 3503–3514. 10.1128/IAI.00602-13.

78. Kremer, N., Voronin, D., Charif, D., Mavingui, P., Mollereau, B., and Vavre, F. (2009). Wolbachia interferes with ferritin expression and iron metabolism in insects. PLoS Pathog. *5*, e1000630. 10.1371/journal.ppat.1000630.

79. Kosmidis, S., Missirlis, F., Botella, J.A., Schneuwly, S., Rouault, T.A., and Skoulakis, E.M.C. (2014). Behavioral decline and premature lethality upon pan-neuronal ferritin overexpression in Drosophila infected with a virulent form of Wolbachia. Front. Pharmacol. *5*, 66. 10.3389/fphar.2014.00066.

80. Marra, A., Masson, F., and Lemaitre, B. (2021). The iron transporter Transferrin 1 mediates homeostasis of the endosymbiotic relationship between Drosophila melanogaster and Spiroplasma poulsonii. microLife *2*, uqab008. 10.1093/femsml/uqab008.

81. Dixon, S.J., Lemberg, K.M., Lamprecht, M.R., Skouta, R., Zaitsev, E.M., Gleason, C.E.,

Patel, D.N., Bauer, A.J., Cantley, A.M., Yang, W.S., et al. (2012). Ferroptosis: an iron-dependent form of nonapoptotic cell death. Cell *149*. 10.1016/j.cell.2012.03.042.

82. Ochsner, U.A., Wilderman, P.J., Vasil, A.I., and Vasil, M.L. (2002). GeneChip expression analysis of the iron starvation response in Pseudomonas aeruginosa: identification of novel pyoverdine biosynthesis genes. Mol. Microbiol. *45*. 10.1046/j.1365-2958.2002.03084.x.

83. Palma, M., Worgall, S., and Quadri, L.E. (2003). Transcriptome analysis of the Pseudomonas aeruginosa response to iron. Arch. Microbiol. *180*. 10.1007/s00203-003-0602-z.

84. Weeratunga, S.K., Lovell, S., Yao, H., Battaile, K.P., Fischer, C.J., Gee, C.E., and Rivera, M. (2010). Structural Studies of Bacterioferritin B (BfrB) from Pseudomonas aeruginosa Suggest a Gating Mechanism for Iron Uptake via the Ferroxidase Center. Biochemistry *49*, 1160. 10.1021/bi9015204.

85. Makui, H., Roig, E., Cole, S.T., Helmann, J.D., Gros, P., and Cellier, M.F. (2000). Identification of the Escherichia coli K-12 Nramp orthologue (MntH) as a selective divalent metal ion transporter. Mol. Microbiol. *35*. 10.1046/j.1365-2958.2000.01774.x.

86. Murdoch, C.C., and Skaar, E.P. (2022). Nutritional immunity: the battle for nutrient metals at the host-pathogen interface. Nat. Rev. Microbiol. *20*. 10.1038/s41579-022-00745-6.

87. Masson, F., Moné, Y., Vigneron, A., Vallier, A., Parisot, N., Vincent-Monégat, C., Balmand, S., Carpentier, M.C., Zaidman-Rémy, A., and Heddi, A. (2015). Weevil endosymbiont dynamics is associated with a clamping of immunity. BMC Genomics *16*. 10.1186/s12864-015-2048-5.

88. Huang, Q., Tang, X., Wang, G., Fan, Y., Ray, L., Bergmann, A., Belenkaya, T.Y., Ling, X., Yan, D., Lin, Y., et al. (2014). Ubr3 E3 ligase regulates apoptosis by controlling the activity of DIAP1 in Drosophila. Cell Death Differ. *21*. 10.1038/cdd.2014.115.

89. Mumbauer, S., Pascual, J., Kolotuev, I., and Hamaratoglu, F. (2019). Ferritin heavy chain protects the developing wing from reactive oxygen species and ferroptosis. PLoS Genet. *15*. 10.1371/journal.pgen.1008396.

90. Vozandychova, V., Stojkova, P., Hercik, K., Rehulka, P., and Stulik, J. (2021). The Ubiquitination System within Bacterial Host–Pathogen Interactions. Microorganisms *9*. 10.3390/microorganisms9030638.

91. Lee, A.K., Detweiler, C.S., and Falkow, S. (2000). OmpR Regulates the Two-Component System SsrA-SsrB in Salmonella Pathogenicity Island 2. J. Bacteriol. *182*, 771. 10.1128/jb.182.3.771-781.2000.

92. Chakraborty, S., Mizusaki, H., and Kenney, L.J. (2015). A FRET-based DNA biosensor tracks OmpR-dependent acidification of Salmonella during macrophage infection. PLoS Biol. *13*, e1002116. 10.1371/journal.pbio.1002116.

93. Brzóstkowska, M., Raczkowska, A., and Brzostek, K. (2012). OmpR, a response regulator of the two-component signal transduction pathway, influences inv gene expression in Yersinia enterocolitica O9. Front. Cell. Infect. Microbiol. *2*. 10.3389/fcimb.2012.00153.

94. Brzostek, K., Brzóstkowska, M., Bukowska, I., Karwicka, E., and Raczkowska, A. (2007). OmpR negatively regulates expression of invasin in Yersinia enterocolitica. Microbiology *153*. 10.1099/mic.0.2006/003202-0.

95. Bernardini, M.L., Fontaine, A., and Sansonetti, P.J. (1990). The two-component regulatory system ompR-envZ controls the virulence of Shigella flexneri. J. Bacteriol. *172*. 10.1128/jb.172.11.6274-6281.1990.

96. Hernández-Gallardo, A.K., and Missirlis, F. (2020). Loss of ferritin in developing wing cells: Apoptosis and ferroptosis coincide. PLoS Genet. *16*, e1008503. 10.1371/journal.pgen.1008503.